M 2025
iza

U.PORTO
FEUP FACULDADE DE ENGENHARIA
UNIVERSIDADE DO PORTO

STUDY OF ALTERNATIVE OER ELECTRODES TOWARDS A MORE SUSTAINABLE ELECTROLYSER DESIGN

FRANCISCO DE ALMEIDA MARTINHO
MASTER THESIS IN CHEMICAL ENGINEERING
PRESENTED TO THE FACULTY OF ENGINEERING
OF THE UNIVERSITY OF PORTO

Master in Chemical Engineering

Study of alternative OER electrodes towards a more sustainable electrolyser design

Master Thesis

of

Francisco de Almeida Martinho

Developed within the course of dissertation

held in

CoLAB NET4CO2 and CEFT/FEUP

Supervisor at FEUP: **Alexandra Maria Pinheiro da Silva Ferreira Rodrigues Pinto**

Joint supervisor(s) at FEUP: **Rui Carlos Barata Ferreira**

Coordinator at CoLAB NET4CO2: **Dânia Sofia Martins Constantino**

August 2025

Acknowledgment

This research was funded by CETPartnership, the Clean Energy Transition Partnership under the 2023 joint call for research proposals, co-funded by the European Commission (GA 101069750) and with the funding organisations detailed on https://cetpartnership.eu/funding-agencies-and-call-modules and developed within the scope of the project “MissãoInterface- 01/C05-i02/2022” under the funding program Recovery and Resilience Plan (PRR).

I would like to thank my supervisors, without them and their work, it wouldn't have been possible for me to carry out my thesis, and I would also like to thank them for the trust they placed in me to continue their work! To Maria Sá, who welcomed me into Net4CO2 from the start, for guiding me through this work, for helping me through the bad times and for all the advice that enabled me to get to the end! To Dânia Constantino, who took on my project in the middle of the year and yet was always willing to help and continue my work, a big thank you for the trust you placed in me.

To Prof. Alexandra Pinto and Rui Ferreira, my academic orientaters, who helped me prepare this thesis and was always there when I needed him.

I would also like to thank Vasco and Milana for taking time out of their projects to help me in the initial stages of this work.

To my girlfriend and my group of friends for helping me to keep my head on straight, for helping me in times of pressure, on good days and bad days throughout these years and for supporting me!

Finally, the most important thanks go to my parents who made it possible for me to be here, who have always been proud of me and who have always encouraged me to want to be better!

Abstract

The rising levels of carbon dioxide (CO_2) emissions around the world, reaching about 41.6 billion tons in 2024, show how important it is to find long-term energy solutions to slow down climate change. Thus, electrochemical CO_2 reduction and water electrolysis offer promising pathways to produce carbon-neutral eFuels and green hydrogen, respectively, supporting decarbonisation efforts in sectors like aviation and heavy transport. However, the oxygen evolution reaction (OER) at the anode, a critical process in these technologies, is still underappreciated and relies on costly and scarce iridium-based catalysts, posing challenges for scalability and economic viability.

This project focused on developing low-cost, sustainable anodes for OER using earth-abundant materials and green synthesis techniques to enhance the sustainability of electrolyser designs. Therefore, the formulation of the catalytic inks was composed mainly of nickel (II) nitrate hexahydrate and increasing quantities of copper (I) oxide. The inks deposited in carbon paper were tested in batch-type electrochemical cells at CoLAB NET4CO2 using cyclic voltammetry to assess their double-layer capacitance, redox reversibility, and OER onset potential. The best performing formulations were then evaluated in an anion exchange membrane (AEM) electrolyser at CEFT/FEUP using polarisation curves under realistic alkaline conditions and results were compared with a catalyst ink prepared using a $NiFe_2O_4$ commercial catalyst.

For the batch tests, all inks showed clear Ni(II)/Ni(III) redox transitions, and a diffusion-controlled behaviour, as confirmed by Randles–Ševčík model. Since all the characteristic results from each ink were the same, the matching point of this analysis was the lowest onset voltage value differentiating the pure nickel ink from the remaining ones.

The AEM electrolyser results additionally validated best performance of the pure nickel formulation, which achieved lower cell voltages (corresponding to a better performance) compared to both commercial $NiFe_2O_4$ and other in-house formulations with copper. It is important to note that the formulations that included copper also showed, compared to the commercial material, better results for lower current densities, although getting worse when achieving higher values of current.

These findings demonstrated that effective OER anodes can be synthesised using simple, low-cost methods without reliance on noble metals or hazardous reagents. The deposition process is scalable and compatible with industrial fabrication, aligning with sustainability and economic goals. Overall, the project provides a promising pathway for the development of alternative anodes suitable for integration into advanced electrolysers aimed at producing renewable hydrogen and/or CO_2-derived fuels.

Keywords: Oxygen evolution reaction (OER), electrolysis, Nickel-based anodes, eFuels

Resumo

A crescente emissão global de dióxido de carbono (CO_2), atingindo uma estimativa de 41,6 mil milhões de toneladas em 2024, sublinha a necessidade urgente de soluções energéticas sustentáveis para mitigar as alterações climáticas. Assim, a redução eletroquímica de CO_2 e a eletrólise da água oferecem caminhos promissores para produzir eFuels neutros em carbono e hidrogénio verde, respetivamente, apoiando os esforços de descarbonização em setores como a aviação e o transporte pesado. No entanto, a reação de evolução do oxigénio (OER) no ânodo, um processo crítico nessas tecnologias, ainda é subestimada e depende de catalisadores caros e escassos à base de irídio, colocando desafios para a escalabilidade e viabilidade económica. Este projeto centrou-se no desenvolvimento de ânodos sustentáveis e de baixo custo para OER, utilizando materiais abundantes na terra e técnicas de síntese ecológicas para melhorar a sustentabilidade dos projetos de eletrolisadores. Consequentemente, a formulação das tintas catalíticas foi composta principalmente por nitrato de níquel (II) hexa-hidratado e quantidades crescentes de óxido de cobre (I). As tintas depositadas em papel de carbono foram testadas em células eletroquímicas de tipo batch no CoLAB NET4CO2, utilizando a voltametria cíclica para avaliar a sua capacidade de dupla camada, a reversibilidade redox e o potencial de início de OER. As formulações com melhor desempenho foram depois avaliadas num eletrolisador de célula de fluxo no CEFT/FEUP, utilizando curvas de polarização em condições alcalinas realistas e comparando-as com uma resultante do catalisador comercial NiFe2O4.

Para os testes batch, todas as tintas apresentaram transições redox Ni(II)/Ni(III) claras, e um comportamento controlado por difusão, como confirmado pelo modelo de Randles-Ševčík. Uma vez que todos os resultados caraterísticos de cada tinta foram os mesmos, o ponto de correspondência desta análise foi o valor mais baixo de tensão de início que diferencia a tinta de níquel puro das restantes. Os resultados da célula de fluxo validaram novamente a superouridade da formulação de níquel puro, que alcançou tensões de célula mais baixas em comparação com o NiFe2O4 comercial e outras formulações internas. É importante notar que as formulações que continham cobre também apresentaram, em comparação com as comerciais, resultados significativamente melhores para densidades de corrente mais baixas, piorando quando atingiram valores mais elevados.

Estes resultados demonstram que podem ser sintetizados ânodos OER eficazes utilizando métodos simples e de baixo custo, sem recurso a metais nobres ou reagentes perigosos. O processo de deposição é escalável e compatível com o fabrico industrial, alinhando-se com os objetivos económicos e de sustentabilidade. No geral, o projeto fornece um caminho promissor para o desenvolvimento de ânodos alternativos adequados para integração em eletrolisadores avançados destinados a produzir hidrogénio renovável e/ou combustíveis derivados de CO_2.

Palavras-chave: Reação de evolução do oxigénio (REO), eletrólise, ânodos à base de níquel, eFuels

Declaration

I hereby declare, under word of honour, that this work is original and that all non-original contributions is indicated and due reference is given to the author and source

July 2025

Index

List of Figures

List of Tables

Notation and Glossary

List of variables

i	Electrical current	A
i_c	Capacitive current	A
E	Potential	V
C_{DL}	Double layer capacitance	F
CL	Catalyst loading	mg cm^{-2}
mf	Mass after catalyst deposition	g
mi	Mass before catalyst deposition	g
A	Area	m^2

Greek Letters

υ	Scan rate
η	Overpotential

Indexes

c	Capacitive
DL	Double Layer
p	Peak
pa	Peak anodic
pc	Peak cathodic

List of Acronyms

AEL	Anion exchange layer
AEM	Anion Exchange Membrane
Ag	Silver
AgCl	Silver Chloride
Au	Gold
Bi	Bismuth
BPM	Bipolar Membrane
CCUS	Carbon Capture, Utilization and Storage
CEL	Cation exchange layer
CEM	Cation Exchange Membrane
CO	Carbon Monoxide
CO2	Carbon Dioxide
Cu	Copper
Cu2O	Copper(I) oxide
CV	Cyclic Voltammetry
DC	Direct Current
DEM	Differential electrochemical mass spectrometry
e-	Electron
eCO2R	Electrochemical CO2 Reduction
Fe	Iron
H2	Hydrogen
H2O	Water
HER	Hydrogen Evolution Reaction
Ir	Iridium

KOH	Potassium Hydroxide
LOM	Lattice oxygen mechanism
NaOH	Sodium hydroxide
Ni	Nickel
Ni(OH)2	Nickel(II) hydroxide
NiOOH	Nickel oxide hydroxide
O2	Oxygen
OER	Oxygen Evolution Reaction
OH-	Ion hydroxide
OLEM	Online electrochemical mass spectrometr
Pt	Platinum
RDE	Rotating disk electrodes
RDS	Rate determing step
Sn	Tin
TOF	Turn of Frequency
TRL	Technology Readiness Levels
XAS	X-ray absorption spectroscopy

1. Introduction

1.1. Framing and presentation of the work

In recent decades, global climate change has been driven largely by the relentless rise in carbon dioxide (CO_2) emissions, a direct consequence of burning fossil fuels. In 2023, fossil-fuel combustion released an estimated 36.8 billion tonnes of CO_2, with total anthropogenic emissions reaching approximately 40.9 billion tonnes [1].

These emissions were projected to climb even higher in 2024, with fossil emissions expected to hit 37.4 billion tonnes and total CO_2 output reaching about 41.6 billion tonnes.

These figures highlight humanity's continued dependence on coal, oil, and natural gas, with just 36 companies now responsible for nearly half of global industrial emissions [2].

The urgent need for transformative action has never been more apparent.

Among the strategies being explored, the electrochemical conversion of CO_2 has emerged as a compelling pathway for reducing greenhouse gas emissions while generating valuable products at mild conditions. Rooted in well-established electrochemical principles, in a typical CO_2 electrolyser the target conversion takes place at the cathode, where CO_2 is reduced, while the anode is responsible for oxidizing water via the oxygen evolution reaction (OER). Traditionally, this requires iridium-based (Ir) catalysts to overcome the sluggish kinetics of water oxidation. However, the high cost and limited availability of noble metals pose serious challenges for scaling up and achieving economic feasibility [3].

Powered by renewable electricity, this setup allows to produce energy-dense molecules such as carbon monoxide, formic acid, and/or hydrocarbons derived from CO_2, thereby transforming a waste gas into high-value chemical feedstocks [4].

Particularly attractive among the range of possible products are liquid hydrocarbon fuels synthesised from renewable hydrogen (H_2) and captured CO_2, commonly referred to as eFuels. These alternative fuels promise the same high energy density and transport convenience as conventional hydrocarbons, but without net CO_2 emissions and are viewed as a practical, near-term option for decarbonising sectors where electrification remains challenging, such as aviation and heavy transport.

At Net4CO_2 CoLAB, the purpose is to accelerate the transition from conceptual science to commercially viable solutions in carbon capture, usage, and storage (CCUS). Also, the aim is to bring competitive and disruptive technologies to the market, contributing meaningfully to a decarbonisdeed future. However, the major bottleneck in deploying CO_2 electrolysers at scale,

however, remains on the anodic side of the cell. While iridium-based catalysts are effective for OER, their scarcity and high cost undermine the economic case for widespread implementation.

This work addresses that challenge by targeting the development of low-cost, sustainable anodes for the OER process, utilizing earth-abundant metals and green synthesis techniques. The main focus was on materials engineered for electrical conductivity, corrosion resistance, and with long-term stability under real operating conditions. These electrodes were synthesised through simple, eco-friendly methods, avoiding harmful reagents and solvent-heavy processes.

The methodological approach begins with bench-scale validation in conventional electrochemical bath cells at Net4CO_2 CoLAB, where screen materials were evaluated based on overpotentials and operational stability. Afterwards, the most promising materials were integrated into an anion exchange membrane (AEM) electrolyser at CEFT/FEUP, allowing to assess their performance under relevant conditions comparing them with anode catalyst commercially available.

The ultimate objective was to elevate these approaches to higher Technology Readiness Levels (TRLs), fostering follow-up projects and attracting commercial interest.

1.2. Presentation of the company

NET4CO2 is a Portuguese collaborative laboratory and a non-profit organisation with its headquarters in Porto. Its principal mission is the development and optimisation of efficient and innovative technologies for capture, utilisation, and storage of CO_2 (CCUS). This thesis concerns a complementary study to the CO2 electrochemical reduction into the utilisation group, for which the Net4CO2 has an innovative concept, the eNetMIX electrolyser, which is already patented (US2019/0010620A1).

Beside technology for electrochemical fuels production from CO_2 conversion, this group is also focused on the development and validation technology for the production of synthetic fuels (via Fischer-Tropsch), including methane from CO2 hydrogenation, and chemicals (like methanol), syngas, biofuels, and CO_2-based materials (cyclic carbonates) with improved efficiency and scalability.

Moreover, NET4CO2 supports industry through laboratory testing, prototype development, deployment of mobile testing units, training, and business development. They are focused in decarbonise the hard to abate industries, like the cement, steel, pulp and paper industries towards the transition to clean energy with tailored studies, and CCU prototypes design and implementation. More detailed information can be consulted on Net4CO2 website (https://www.net4co2.pt).

Regarding the tests in water electrolyser. They were carried out at the Transport Phenomena Research Centre (CEFT) in FEUP. CEFT is a research unit dedicated to investigating heat, mass, and momentum transport processes, serving as a link between chemical and mechanical engineering. The centre is organised into two main sub-groups: the energy group, which concentrates on cleaner fuel production and the hydrogen economy, and the Fluids group, which specialises in the study of complex, smart, multiphase, and biological fluids [5].

1.3. Contribution of the author to the work

The research presented in this dissertation was developed in collaboration with two research institutions: The NET4CO2 CoLAB and the CEFT (Transport Phenomena Research Centre). My contribution at NET4CO2 involved the conceptual development of the proposed processes, supported by an extensive literature review.

In this work, I optimised the ink deposition methodology and tested for the first time nickel electrodes for water electrolysis as a case study. Afterwards, I even study the addition of copper in the formulation of the inks to see if it provides better or worse results comparing with the ones previously obtained before the project. In an overall point of view, the results were positive.

In short, this work has paved the way for optimising the process at the anode. This optimisation is of the utmost importance as the anode process is complementary to both CO_2 electrolysis to produce e-fuels and water electrolysis for the production of hydrogen (H_2), contributing to the advancement of more sustainable energy technologies.

1.4. Organisation of the dissertation

This dissertation provides a logical and comprehensive exploration of the development of alternative anodes for the oxygen evolution reaction (OER) to create a more sustainable electrolyser design.

Chapter 1 introduces the motivation and context of the work by detailing the technological and climate-related challenges that underscore the necessity of novel OER catalysts. The chapter also presents the institutions involved and the author's specific contributions.

Chapter 2 presents the scientific background and current state of research, covering topics such as water and CO_2 electrolysis, key electrochemical reactions (e.g., HER and OER), principles of catalyst design, membrane technologies, and the comparative performance of reactor configurations. The chapter concludes by identifying current limitations and knowledge gaps that motivate the experimental work.

Chapter 3 describes the materials and methods used for the study, including the design and preparation of catalytic inks, the specifications of the electrodes and membranes, and the electrochemical setups: batch and flow-type cells. The chapter also outlines the characterizsation techniques employed, such as cyclic voltammetry and polarisation curves.

Chapter 4 presents the results obtained from batch and flow cell experiments. It provides a detailed analysis of double-layer capacitance, redox behaviour, and the overall catalytic performance of different ink formulations through batch tests. The AEM electrolysis tests via polarisation curves include a benchmarking of the formulations against the commercial reference $NiFe_2O_4$.

Chapter 5 synthesises the key findings into final conclusions, highlighting the strengths and limitations of the proposed materials.

Chapter 6 assesses the work against the stated objectives and its contribution to the United Nations Sustainable Development Goals. It also discusses any additional work carried out.

Finally, the references, annexes, and appendices provide the supporting data and methodological details that are essential for the reproducibility and transparency of the study.

2. Context and State of the art

Electrochemistry is a pillar of the global transition toward a sustainable, low-carbon energy landscape. By facilitating the direct conversion of electrical energy particularly from renewable sources into chemical fuels, it fosters the production of green hydrogen through water electrolysis, a pivotal technology for decarbonisation and achieving climate objectives.

In this context, the hydrogen evolution reaction (HER) and the oxygen evolution reaction (OER) function in a coordinated manner where HER produces H_2 while OER completes the cycle by generating O_2. The optimisation of these complementary half-reactions is imperative for enhancing efficiency and reducing costs. Concurrently, CO_2 electrochemical reduction (eCO_2RR) provides a method for the transformation of captured carbon into valuable chemicals, integrating oxygen evolution reaction (OER) on the anode and thereby accelerating decarbonisation efforts.

Among the suite of electrochemical processes vital to our climate goals, carbon dioxide (CO_2) reduction and water electrolysis stand out for their versatility and impact. In the context of water electrolysis, HER plays a pivotal role in facilitating the generation of pure H_2, while OER, the focal point of this study, governs the efficiency and stability of the entire system.

In the ensuing sections, an in-depth examination of these types of electrolysis will be conducted, followed by a more comprehensive exploration of OER. The discussion will encompass catalytic strategies and performance metrics that are indispensable for the large-scale decarbonisation.

2.1. CO_2 electrolysis

The electrochemical reduction of carbon dioxide (CO_2 electrolysis or eCO_2RR) offers a promising avenue for converting CO_2, a prevalent greenhouse gas, into valuable chemicals by using electricity under mild conditions. This route not only stores surplus renewable energy but also aligns with carbon mitigation goals, forging a pathway toward a circular, carbon-neutral economy [6].

In a typical CO_2 electrolyser cell, CO_2 is fed to the cathode, where it undergoes reduction, while at the anode, water is oxidised as a process known as the oxygen evolution reaction (OER) to supply protons and electrons necessary to sustain the cathodic reaction. These protons usually traverse an ion-exchange membrane, completing the ionic circuit within the cell [7, 8].

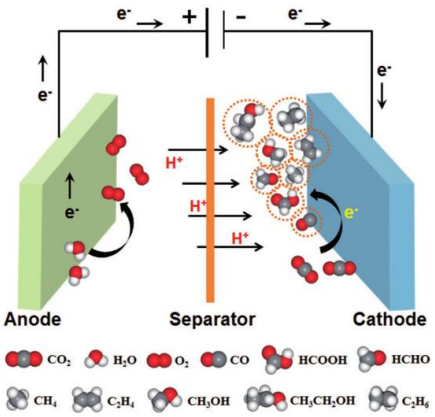

Figure 1 - Schematic diagram of the electrochemical CO2 reduction reaction system [9].

Usually at the cathode the most common electrocatalysts such as silver, gold, tin, bismuth or copper are used to activate and reduce CO_2 into valuable chemicals and fuels such as carbon monoxide, formate, methane, ethylene and ethanol. Each catalytic material directs the reaction toward distinct products formation: Ag and Au exhibit high selectivity for CO; Sn and Bi favour formate, while Cu is unique in producing multi-carbon hydrocarbons like ethylene and alcohols like methanol and ethanol, among others. The exact distribution of products depends on several factors including the catalyst binding affinities, operation conditions, the interactions with the electrolyte, its morphology and electronic structure [10].

On the other side of the cell, at the anode, there is water oxidation that generates O_2, electrons, and protons. The catalyst used on the anode must efficiently catalyse the oxygen evolution reaction (OER) while resisting degradation in the oxidative, often high-pH environment. Therefore, the catalyst dissolution and structural degradation remain key challenges, as highlighted in recent studies of anode stability [7].

The electrolyte and membrane also play a pivotal role in controlling the ion transport, pH and most importantly, the CO_2 availability. Furthermore, gas-diffusion electrodes help enhance CO_2 transport to the reactive sites, enabling higher current densities and improved efficiency.

2.2. Oxygen evolution reaction (OER)

The oxygen evolution reaction, OER, is a key anodic process in electrochemical devices used for clean energy conversion, such as water splitting or metal–air batteries. OER often serves as the complementary anodic reaction in full-cell configurations for CO_2 and N_2 electrochemical reduction or even for hydrogen evolution reaction. It has a vital role in transforming water or hydroxide to molecular oxygen through the loss of four electrons and pairing with cathodic half-reactions in various technologies. Despite the conceptual straightforwardness, OER is plagued by slow kinetics because of the intricate multi-step process, including bond rearrangements

and several proton–electron transfers. Consequently, large overpotentials need to be applied to push the reaction at significant rates, stimulating rigorous research to design efficient and stable electrocatalysts [11].

In alkaline conditions, the overall OER reaction can be expressed as equation 1:

$$4\,OH^- \rightarrow O_2 + 2\,H_2O + 4e^- \quad (1)$$

Two principal mechanisms are usually involved in this transformation: the adsorbate evolution mechanism (AEM) and the lattice oxygen mechanism (LOM). The AEM operates via sequential adsorption and transformation of intermediates such as ~OH, ~O, and ~OOH on the catalyst surface. The O–O bond formation, often the rate-determining step (RDS), may occur through nucleophilic attack of hydroxide on ~O or through coupling of adjacent ~O species. By contrast, the LOM involves direct participation of lattice oxygen atoms, which may form oxygen–oxygen bonds through vacancy dynamics or radical pathways. While LOM can exhibit enhanced activity, it is typically associated with structural instability and irreversible changes to the catalyst surface.

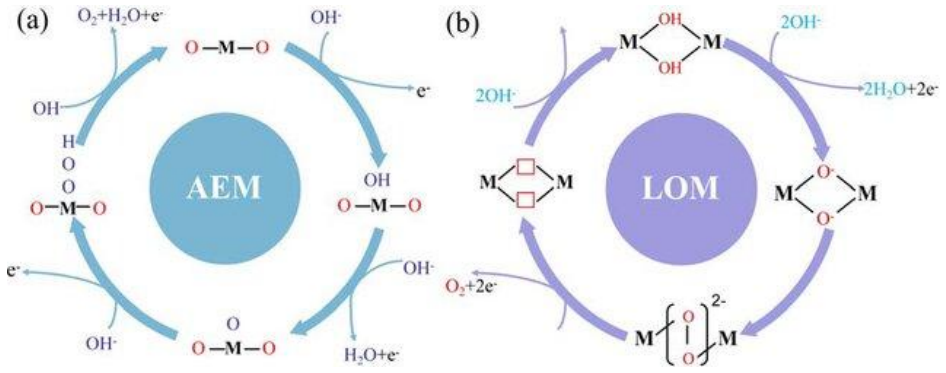

Figure 2 - Oxygen evolution reaction mechanism. (a) Traditional adsorption evolution mechanism. (b) Lattice oxygen precipitation mechanism [12].

The determination of which mechanism dominates is often complex and dependent on pH, potential, catalyst composition, and electrolyte composition. In-situ spectroscopic methods such as X-ray absorption spectroscopy (XAS), Raman, and online electrochemical mass spectrometry (OLEMS) are indispensable tools for capturing intermediate species and tracing oxygen isotope labels in real time [13].

The development of mechanistic insights, facilitated by advanced in situ techniques, has led to a more profound comprehension of the factors that govern the OER. To further refine this understanding, it is imperative to examine the nature of the active sites and their electronic

structures, the fundamental electrochemical driving forces and associated kinetics, as well as the key performance metrics utilised to evaluate catalytic activity. These interconnected aspects form the basis for rational catalyst design and comparative benchmarking across different materials and operating conditions.

2.2.1 Active Sites and Electronic Structure

The catalyst active phase is frequently different from the as-synthesised material, as many metal hydroxides or oxides undergo electrochemical reconstruction under anodic conditions. For example, $Ni(OH)_2$ can oxidise to NiOOH, while Fe-doped Ni structures often form layered oxyhydroxides with high OER activity. The nature of the redox-active centre, whether metal-centred (e.g., Ni^{3+}/Ni^{4+}) or ligand-centred (e.g., oxyl radicals on oxygen ligands), depends on the catalyst's electronic structure and bonding configuration [14].

2.2.2 Electrochemical Driving Force and Kinetics

The driving force for OER is the applied electrochemical potential, which impacts both the activation energy of the reaction and the surface coverage of key intermediates. This potential is composed of both electrostatic and chemical contributions to the total electrochemical potential of species at the interface [14].

2.2.3 Electrocatalytic Performance Metrics

Catalyst performance is traditionally benchmarked using the overpotential at a fixed current density, most commonly 10 $mA \cdot cm^{-2}$, which is considered the minimum requirement for achieving 10 % solar-to-hydrogen efficiency [11].

However, this geometric activity does not reflect the intrinsic catalytic properties, as it is highly dependent on loading, porosity, and substrate effects. To address this, several normalisation strategies are employed:

- Mass activity ($A \cdot mg^{-1}$ catalyst) which reflects the catalyst utilisation efficiency.
- Specific activity ($A \cdot cm^{-2}$ ECSA) that relates current to electrochemically active surface area.
- Turnover frequency (TOF) measures the number of oxygen molecules produced per active site per second.
- Faradaic efficiency, often measured via differential electrochemical mass spectrometry (DEMS), assesses the selectivity of the catalyst toward OER versus parasitic redox processes.

Each metric offers unique insight, but none are universally intrinsic. Mass transport limitations, catalyst utilisation, and electrode architecture can all bias the measurements. As such, best

practices dictate reporting multiple normalised activities and explicitly detailing electrode configuration and testing conditions [11, 13-15].

2.2.4 Experimental Design and Challenges

Successful OER characterisation is not just dependent on the catalyst but also on careful experimental design. The standard setup includes a three-electrode cell with a reference electrode (e.g., Ag/AgCl, referenced HER), a counter electrode (often inert, e.g., Pt), and a working electrode onto which the catalyst is loaded. The substrate selection must be carefully chosen. Although glassy carbon is common due to its inert nature, it is corroded at OER-relevant potentials to form CO/CO_2 and insulating oxides that distort current measurements. Alternatives like titanium felt, nickel foam, and gold are more stable but vary in conductivity, cost, and surface interaction with the catalyst [11].

Bubble formation is among the main issues in OER testing. When oxygen evolves at the anode, gas bubbles can adhere to the catalyst surface, occlude active sites, and increase local resistance. All reduce apparent activity and can eventually impair the electrode. Rotating disk electrodes (RDE), ultrasonication, and floating electrode geometries with vacuum suction are a few of the techniques that have been conceived to minimise bubble accumulation and promote mass transport [15].

2.3. Water electrolysis

Although the primary objective of this work is to study and enhance the OER process as a complement to CO_2 electrochemical reduction, the experimental tests will be conducted in water electrolysis framework to validate the catalytic materials and evaluate their performance. Water electrolysis was selected as the case study due to its technological maturity and the well-established operating conditions available in the laboratory environment at CEFT. This approach allows for a more controlled and reliable assessment of the developed materials, ensuring that the observed electrochemical behaviour and catalytic activity are not influenced by the additional complexities inherent to CO_2 reduction systems. In doing so, it becomes possible to isolate and optimise the OER performance, which is critical for both water splitting and as a half-reaction in integrated CO_2 electrolysis configurations.

Water electrolysis is an archetype of electrochemical conversion, wherein water molecules are split into their constituent gases, hydrogen (H_2) at the cathode and oxygen (O_2) at the anode, through the application of an external direct current voltage. The overall cell reaction is presented in equation 2:

$$2\,H_2O\,(l) \rightarrow 2\,H_2(g) + O_2(g) \quad (2)$$

Under standard conditions, the thermodynamic minimum potential required is 1.23 V, though in practice the applied cell voltage ranges between approximately 1.5 and 2.0 V to surmount kinetic activation barriers and resistive losses, especially the sluggish OER at the anode.

2.4. Membranes

In electrochemical systems, membranes play a fundamental role in separating the anodic and cathodic compartments while ensuring ionic conductivity across the cell. The ideal membrane must offer high ionic selectivity, low resistance, and chemical stability under operating conditions. Three main categories of ion exchange membranes are commonly used in electrochemical systems: bipolar membranes (BPMs), cation exchange membranes (CEMs) and anion exchange membranes (AEMs). Figure 3 shows schematically this membranes.

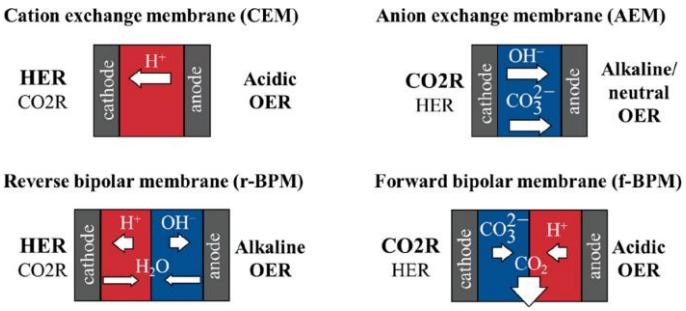

Figure 3 - Schematics of the ion transport processes through different membranes during CO2 electrolysis in membrane-separated CO2 electrolyser cells. The reactions favoured due to the local chemical environment of the electrode, defined by the membrane, are highlighted in bold [16].

BPMs are multilayered membranes formed by laminating a cation exchange layer (CEL) and an anion exchange layer (AEL). Their main function is to allow for the regeneration of water at the interfacial layer via water dissociation into H^+ and OH^-, effectively enabling the maintenance of different pH environments in the anode and cathode compartments. This can be especially advantageous in systems where product crossover or pH sensitivity is a concern. However, BPMs typically require higher operating voltages due to the overpotential associated with water dissociation at the membrane interface [17].

2.4.1 Cation Vs Anion Exchange Membranes (CEM vs AEM)

CEMs contain fixed negatively charged groups, such as sulfonic acid moieties, that allow the passage of positively charged ions (e.g., H^+, K^+). The most widely used CEM in electrochemical

applications is Nafion®, a perfluorosulfonic acid (PFSA)-based membrane, due to its high proton conductivity and mechanical robustness. However, Nafion® and similar membranes tend to acidify the cathode interface and enhance hydrogen evolution reaction (HER), thus limiting CO_2 reduction selectivity [18].

Anion Exchange Membranes (AEMs) are a specialised class of ion-conductive polymeric materials designed to selectively transport anions such as hydroxide (OH^-), bicarbonate (HCO_3^-), and carbonate (CO_3^{2-}) through their structure while preventing the crossover of gases and neutral species. These membranes play a central role in a wide range of electrochemical energy conversion systems, most notably in CO_2 electrolysis and alkaline AEM water electrolysis [18].

Although the same underlying principles of anion transport apply in both applications, the physicochemical environment, ion transport mechanisms, and operational challenges differ significantly, imposing distinct demands on membrane performance and stability.

In their essence, AEMs are constructed from a polymeric backbone, typically based on materials such as poly(phenylene oxide), poly(aryl ether sulfone), or polyolefins, functionalised with fixed cationic headgroups (commonly quaternary ammonium, imidazolium, or phosphonium) [19].

These positively charged sites form hydrated ion channels that interact electrostatically with mobile anions in the electrolyte. The migration of anions through the membrane is primarily governed by electrostatic attraction, ion-exchange diffusion, and field-driven conduction, all of which depend strongly on the hydration state, the structure and connectivity of ionic domains, and the thermodynamic stability of the membrane matrix.

In CO_2 electrolysis, the role of the AEM extends beyond mere ion conduction. The reduction of CO_2 at the cathode typically generates OH^- as a by-product. This OH^- migrates through the AEM toward the anode, where it participates in the oxygen evolution reaction (OER). However, in the presence of CO_2, hydroxide rapidly reacts to form bicarbonate and carbonate species. These additional anions, although still mobile within the membrane, exhibit lower conductivity and tend to accumulate, leading to performance degradation through carbonate precipitation, increased area-specific resistance, and pH imbalance [18].

As a result, AEMs for CO_2 electrolysis must exhibit high selectivity for OH^- transport, while also withstanding chemical degradation from hydroxide and carbonate attack.

In contrast, AEMs used in alkaline water electrolysis are exposed to a simpler ionic environment dominated by OH^- and are often operated at elevated temperatures (typically 60–80 °C). The real challenges for AEMs in this application lies in maintaining mechanical and chemical stability under these conditions. Thus, at such temperatures, OH^- become more aggressive, accelerating degradation mechanisms like Hofmann elimination and nucleophilic substitution of the

quaternary ammonium headgroups which can break down the functional headgroups and compromise membrane integrity [19, 20].

Consequently, AEMs for water electrolysis prioritise chemical stability, thermal durability, and mechanical robustness to sustain prolonged operation under harsh alkaline conditions [21, 22].

2.5. Cathode catalysts

The cathode catalyst is a key determinant of performance, but its optimal composition depends heavily on whether the target reaction is water electrolysis or CO_2 electrolysis.

In water electrolysis, the cathode drives the hydrogen evolution reaction (HER), which benefits from highly active noble metals like Pt/C that minimise activation overpotentials. However, the alkaline environment of AEMs allows for the effective use of non-noble alternatives such as NiFeCo and NiMo, which, despite showing slightly higher overpotentials, offer promising stability and cost advantages.

In contrast, CO_2 electrolysis involves the selective reduction of CO_2 to value-added products such as CO, formate, or hydrocarbons. This process requires catalysts with entirely different surface properties and reaction pathways; copper-based materials, including metallic Cu and Cu_2O, are most employed due to their unique ability to promote C–C coupling and hydrocarbon formation.

Table 1 - Comparations between cathode catalysts for Water and CO2 electrolysis

Process	Catalysts	Advantages	Observations	References
Water electrolysis (HER)	Pt/c; NiMo	• **Pt/C** – minimal activation overpotential • **NiMo** - ultra-low overpotential • **NiFeCo** – non-noble,stable, cost effective	• **NiMo foam**: 17 mV→10 mA cm^{-2}, 98 mV→ 400 mA cm^{-2} • **Y-NiMo/MoO_2**: 189 mV → 2 A cm^{-2}; 2500 h stability	Ádam Vass et al. [23]
CO_2 electrolysis (eCO_2RR)	Cu_2O	• **Cu/OD-Cu**: enables C–C coupling to hydrocarbons/C_2^+ products	• **OD-Cu**: up to 70 % selectivity for C_2^+ products; structurally dynamic with residual oxygen	Lien-Chun Weng et al. [24]

Other materials like silver and tin are preferred for producing CO and formate, respectively, while platinum is generally avoided as it favours HER over CO_2 reduction. Thus, while both processes occur under similar alkaline conditions, the catalyst requirements diverge substantially. HER catalysts prioritise overpotential minimisation and hydrogen selectivity, whereas CO_2 electroreduction catalysts focus on binding strength, intermediate stabilisation, and product selectivity.

2.6. Anode catalysts

The development of efficient, stable, and low-cost anode catalysts for the Oxygen Evolution Reaction (OER) remains central to the advancement of water and CO_2 electrolysis technologies. The OER is a kinetically sluggish favour-electron process and demands highly active materials that can sustain operation under harsh electrochemical environments. The current literature identifies two main families of OER catalysts: noble metal oxides and transition metal-based oxides and (oxy)hydroxides.

2.6.1 Noble Metal Oxides (IrOx, RuOx)

Noble-metal oxides such as IrO_2 and RuO_2 are benchmarks for alkaline OER, offering exceptional activity but still facing trade-offs between performance and cost/stability.

In 1 M–4 M KOH (pH 13–14), RuO_2 achieves low overpotentials ranging from 270 to 280 mV at 10 mA cm^{-2} while remaining structurally stable during operation. This assertion is substantiated by operando XAS revealing that its oxidation state remains largely unchanged during cycling. Besides, mechanically speaking RuO_2 follows the conventional 4-electron adsorbate pathway (forming M–OH, M–O, M–OOH), with the transformation of M–O to M–OOH identified as the rate-limiting step [25].

In a similar manner, IrOx (hydrated IrO2) demonstrates excellent kinetics in alkaline media, exhibiting comparable overpotentials. Recent studies report an overpotential of approximately 270 mV at 10 mA cm^{-2}, with the presence of lattice water facilitating dynamic oxygen exchange and enhancing durability. This enhancement enables sustained operation at 1 A cm^{-2} and a cell voltage of approximately 1.77 V at 60°C. In alkaline electrolyzers, IrOx has been demonstrated to facilitate low charge-transfer resistance across high current densities [26].

2.6.2 Non-Noble Transition Metal Oxides

The shift toward earth-abundant alternatives has led to the exploration of Ni-, Co-, and Fe-based oxides. Among them, NiFeOx consistently emerges as one of the most active and stable catalysts in alkaline environments. It exhibits a low overpotential ($\eta_{10} \approx 0.35$ V) and high turnover frequency, attributable to synergistic electronic interactions between Ni and Fe

centers. Co-based materials like CoFeOx and CoPi (Co phosphate) also demonstrate comparable activity with moderate stability [27].

These systems are particularly advantageous for integration into Anion Exchange Membrane (AEM) and CO_2 electrolysis cells due to their compatibility with alkaline media. In Figure 4 the overpotential of various OER electrocatalysts are compared highlighting the superior performance between them [16].

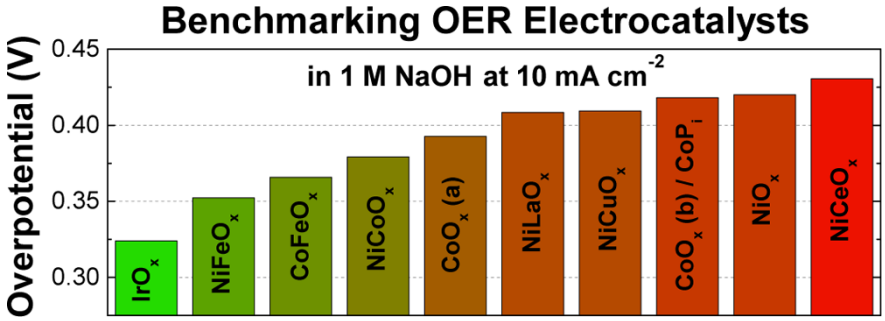

Figure 4 - Comparative benchmarking of OER catalysts by McCrory et al. showing overpotentials and geometric current densities in 1 M NaOH [27].

The electrochemical environment, most importantly pH, plays a decisive role in catalyst stability. IrOx is stable in acidic conditions but dissolves in alkaline media over long durations. In contrast, NiFeOx, NiCeOx, and Co-based catalysts are stable under alkaline conditions but degrade rapidly in acidic or neutral electrolytes.

In CO_2 electrolysis, where the anode is exposed to carbonate/bicarbonate-rich near-neutral media, catalyst stability becomes more complex. Ni- and Co-based oxides are susceptible to carbonation and dissolution, particularly at elevated potentials. Thus, despite promising alkaline performance, their deployment in CO_2 electrolysis requires mitigation strategies such as protective coatings or dynamic electrolyte buffering [16].

2.7. Reactors Design

Electrochemical reactor design is a cornerstone in the advancement of electrolysis technologies, directly impacting efficiency, scalability, and applicability across various sectors, including energy conversion, environmental remediation, and chemical synthesis. The evolution from traditional batch systems to sophisticated flow reactors underscores the importance of reactor configuration in optimizing electrochemical processes.

2.7.1 Batch Vs Flow Reactors

Batch electrochemical reactors operate in discrete cycles, where a fixed volume of electrolyte is processed over time. This setup allows for precise control over reaction conditions, making

it ideal for laboratory-scale experiments, kinetic studies, and the synthesis of high-value chemicals. In batch reactors, the concentration of reactants and products changes over time, necessitating careful monitoring to optimise reaction conditions. These systems facilitate detailed kinetic studies and the development of reaction models since they enable us to acquire data over time under different operating conditions. However, batch reactors face limitations in scalability and may exhibit inefficiencies in mass and heat transfer, which can affect reaction rates and energy consumption.

In contrast, flow electrochemical reactors operate by continuously introducing reactants and removing products, facilitating steady-state conditions. This continuous operation enhances mass and heat transfer, leading to improved reaction efficiency and scalability [28]. Flow reactors often employ configurations such as parallel plate designs or microfluidic channels, which provide high surface-area-to-volume ratios and precise control over reaction conditions. The integration of flow systems allows for seamless scaling from laboratory to industrial applications, making them suitable for large-scale production processes [29]. Advanced designs incorporate features like static mixing and microstructuring to enhance mass transfer and reaction kinetics. However, the complexity of design and the need for sophisticated control systems can pose challenges in implementation [30].

The transition from batch to flow systems involves a fundamental shift in reactor design and operation. Flow reactors enable the integration of electrochemical processes with other unit operations, facilitating continuous production lines and real-time monitoring. Moreover, the ability to maintain steady-state conditions in flow systems leads to consistent product quality and efficient resource utilisation. These advantages make flow reactors particularly advantageous in electrolysis processes requiring high throughput and efficiency, such as water splitting for hydrogen production and the electrochemical synthesis of organic compounds [31].

The design of electrolysis systems is of paramount importance, particularly with regard to the efficiency, scalability, and real-world viability of the resulting systems. Batch reactors are recognised for their operational simplicity and precise control over temperature, pressure, and residence time. These reactors excel in small-scale and exploratory applications, including early-stage catalyst screening and detailed reaction optimisation.

The adaptability of these conditions enables researchers to make adjustments during the course of a study, accommodating the presence of varying reactants or pathways. This capacity is of paramount importance for the development of methods in the domains of pharmaceutical and specialty chemical synthesis.

Nonetheless, batch systems are subject to inherent constraints as reactions progress. These constraints include reactant depletion and by-product buildup, which can lead to deterioration in mass transport. This deterioration often results in a decline in current efficiency over time.

Furthermore, the formation of gas evolution bubbles at electrodes, a well-documented phenomenon with deleterious effects on energy and mass transfer, leads to the accumulation of these bubbles over time. This, in turn, results in the escalation of overpotentials and the deterioration of energy efficiency. The mitigation of these issues necessitates the periodic reactivation of catalysts or the implementation of cleaning protocols [32].

Conversely, flow reactors are gaining popularity for their application in continuous and large-scale electrochemical production, a preference that can be attributed to their inherent superiority in terms of mass and heat transfer characteristics. The utilisation of narrow inter-electrode gaps, frequently measuring less than 1 mm, in conjunction with a high electrode surface-area-to-volume ratio, facilitates the attainment of elevated current densities and diminished resistive losses [33].

The system operates in a steady-state condition, whereby fresh reactants are continually supplied while existing products and bubbles are systematically expelled. This continuous process serves to prevent catalyst fouling and ensure the system's optimal functionality. Indeed, techno-economic assessments consistently demonstrate that continuous-flow processes often exhibit significantly lower energy consumption, reduced water use, and more sustainable mass utilisation when compared to batch operations [34].

A salient benefit emerges from the dynamics of bubbles. In flow systems, evolving bubbles are rapidly transported, either by the flow or through coalescence and detachment. This behaviour has been demonstrated to enhance electrolysis efficiency by over 30 % [35].

Further computational analyses indicate that bubble-induced convection and buoyancy-driven mixing are the predominant factors in mass transfer near electrodes, thereby facilitating more consistent Faradaic efficiency.

In water electrolysis, recent advancements in the field of engineering, exemplified by the development of microstructured flow channels featuring biomimetic or turbulence-promoting geometries, have demonstrated a substantial enhancement in mass transfer rates. In comparison with conventional cells, these innovations have shown a remarkable improvement, effectively doubling the rate of mass transfer. Microreactors that demonstrate high performance in the domain of organic electrosynthesis have been shown to achieve conversion rates of 100 %, along with current efficiency levels of approximately 90 %, even under conditions of current density as high as 2500 A m^{-2} [36].

A notable advantage of flow reactors is their modular architecture, which facilitates scale-up processes. Configurations such as filter-press cells and membrane-electrode assemblies (MEAs) permit variable channel dimensions and the possibility of gas/liquid segregation. This

modularity facilitates incremental volume increases without necessitating redesign of the core cell, a notable improvement over the often unwieldy batch-scale up process.

However, translating batch methods into continuous flow processes is not without its challenges. Research has identified critical parameters such as inter-electrode spacing, electrolyte concentration, and current density that necessitate precise calibration to ensure the conservation of current and energy efficiencies.

2.8. Challenges and Research Gaps

In the context of alkaline oxygen evolution, the accurate quantification of ECSA, remains a challenging endeavor for mixed-metal oxides. In contrast to noble metals, where CO-stripping serves as a reliable probe, oxide surfaces lack such definitive redox markers. Consequently, conventional methods such as double-layer capacitance frequently underestimate or misrepresent true ECSA [37].

The issue is further combined by the instability of the catalyst and surface reconstruction during OER. Ni–Fe or Co–Mn oxide films often undergo a transformation into oxyhydroxides under conditions of alkaline operation and such transformations have the capacity to induce dynamic changes in the composition of the active site and the conductivity of the material, thereby rendering it challenging to decouple intrinsic activity from emergent surface states.

These evolving surfaces are further prone to metal leaching and incomplete redox cycling. The dissolution of Fe, Co, or Mn atoms from the lattice during extended high-potential operation can lead to a significant alteration in the catalyst's composition mid-reaction. The quantification of the interplay between metal loss and lattice oxygen participation remains an area of research [38].

Mechanically, uncertainties persist under conditions of elevated pH since alkaline OER involves OH^- adsorption and multiple electron transfers. However, the rate-determining step appears to shift with pH and catalyst structure. Tafel slopes and reaction orders exhibit substantial variation across the pH range from 12 to 14, a phenomenon that complicates kinetic modeling across diverse oxide systems [39].

Additionally, the potential involvement of lattice oxygen-driven mechanisms (LOM) remains a subject of ongoing discussion and research. While some evidence suggests that lattice O atoms may directly participate in O–O bond formation (alongside or instead of the conventional adsorbate-evolution path), the balance between these pathways changes with composition, potential, and pH. To have a better understanding of this matter, further isotope tracing and coupling with dissolution are required.

3 Materials and Methods

3.1 Materials

3.1.1 Counter and reference electrodes

For electrochemical batch experiments, a 99.9 % platinum wire counter electrode supplied from Redox.me with a total length of 250 mm, 50 mm active zone, and a wire diameter of 0.6 mm was used. Intended to serve as the auxiliary electrode, it completes the electrical circuit by allowing current flow without interfering with the primary redox reactions. Silver/silver chloride (Ag/AgCl) reference electrode measuring 30 mm in length from Redox.me, was also employed to give stable and well-defined reference potential during the measurements. Both electrodes were cleaned using ultrapure water before each experimental trial.

3.1.2 Working electrode

For the same tests, the working electrode used was Toray carbon paper TGP-H-060, which was acquired from Thermo Scientific, and consisted of 1.6 cm × 1.6 cm squares, tailored to the cell configuration. The material is recognised as a highly conductive and porous carbon substrate commonly utilised in electrochemical applications because of its high electrical conductivity, chemical stability, and mechanical strength. Its microporous nature allows for the permeation of gases and enables efficient interaction between the electrode and the electrolyte. In this case, carbon paper serves as the substrate for the catalyst deposition, offering a stable and inert surface for subsequent ink deposition.

3.1.3 Catalytic ink formulation

In this project, the central focus is the development of catalytic inks aimed at enhancing the performance of electrochemical systems through the use of abundant, corrosion-resistant, and highly conductive materials, while also favouring green and scalable preparation methods suitable for industrial application. The testing strategy follows a two-step approach: catalytic inks are first evaluated in batch electrochemical cells, and the most promising formulations are subsequently tested in AEM electrolysers for more advanced performance assessment.

The first ink formulation consisted of nickel supported on silica/alumina, Ni/SiO_2-Al_2O_3 with approximately 65 wt.% metal loading from Merck (Product No. 208779). Nickel (II) nitrate hexahydrate provided from Analar NORMAPUR was also tested, as alternative to the first catalyst, due to its superior ionic conductivity and improved solubility in the ink preparation process. Based on this precursor, four different ink compositions were formulated: i) 100 % Nickel(II) nitrate hexahydrate, and mixtures containing ii) 95 %, iii) 90 %, and iv) 85 % of this

salt combined with 5 %, 10 %, and 15 % of Copper(I) oxide (97 % Cu + Cu_2O assay, Thermo Scientific), respectively.

Each ink formulation was prepared using a 70:30 catalyst-to-Nafion mass ratio, and a 3 wt.% total solids concentration (catalyst + Nafion dispersion, 5wt.% from *Alfa Aeser* (USA)), with the remaining 97 % consisting of isopropanol (IPA) (provided from Sigma-Aldrich) as the solvent. Prior to deposition, the inks were homogenised in an ultrasonic bath for 30 minutes. The final suspension was then deposited onto the carbon paper substrate by airbrushing using a DEXTER DX-1839 aerography pistol, while the substrate was placed on a heating plate maintained at 60 °C to ensure rapid solvent evaporation and uniform film formation.

The catalyst deposition was prepared so that the catalyst loading was close to 2 mg·cm-2. The electrode was weighed before and after partial depositions, allowing to calculate the actual loading by mass difference after each deposition until we achieve a value close to the desired.

The catalyst loading was calculated through equation 3 and the deposition of the catalysts is demonstrated by Figure 5.

$$CL = \frac{(m_f - m_i) \cdot 0.7 \cdot 1000}{A} \left(\frac{\boldsymbol{mg}}{\boldsymbol{cm^2}}\right) \quad (3)$$

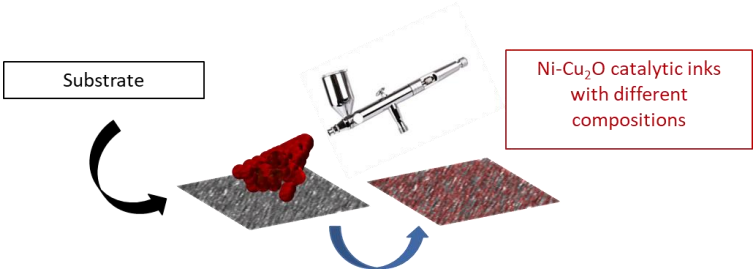

Figure 5 - Schematic representation of the electrodes preparation

3.1.4 Electrolyte

The electrolyte used in the electrochemical assays was prepared by dissolving potassium hydroxide (KOH) pellets, of analytical reagent grade from Fisher Chemical, in ultrapure water to obtain a 1 M KOH solution. The solution was mixed thoroughly to ensure complete dissolution and homogeneity before use in the batch cell setup.

In electrochemical systems, KOH is widely used as an alkaline electrolyte due to its high ionic conductivity and chemical stability. The 1 M KOH solution provides hydroxide ions OH^- necessary to support charge transport and maintain the required alkaline environment for redox

reactions, particularly in studies involving OER. Its compatibility with a broad range of electrode materials makes it a standard choice in alkaline electrochemistry.

3.1.5 Cathode substrate

The cathode used in this study was a carbon cloth substrate with a thickness of 0.410 mm. Carbon-based electrodes are commonly employed in alkaline electrolysis due to their high electrical conductivity, porosity, and mechanical flexibility, which together facilitate effective gas removal, water distribution, and electron transport. These properties make carbon cloth particularly suitable for supporting the hydrogen evolution reaction (HER) under alkaline conditions.

3.1.6 Anode substrate

A different gas diffusion layer was used for the electrolyser compared to the one used in the batch cell tests. The anode used in this stage was a stainless steel 316L (SS 316L) felt with a thickness of 0.600 mm. This material was selected for its excellent corrosion resistance in alkaline media, combined with robust mechanical properties and good electrical conductivity. The felt structure provides a high surface area, which is beneficial for enhancing reaction kinetics.

Each stainless steel electrode was prepared and coated using the same procedure used previously in the batch cell.

3.1.7 Membrane

The membrane used in the electrolyser was the Fumasep FAS-50, a commercially available anion exchange membrane with a nominal thickness of 50 µm and an OH^- ionic conductivity typically around 20–25 $mS \cdot cm^{-1}$ at 30 °C in 1 M KOH, as reported by the manufacturer Fumatech. The membrane has a reinforced structure based on an undisclosed polymeric matrix, optimised for chemical resistance and mechanical stability in alkaline environments.

The FAS-50 functions by selectively transporting hydroxide ions OH^- across the membrane plane, while simultaneously preventing gas crossover and maintaining electrical insulation between the electrodes. Its area-specific resistance is typically below 3 $\Omega \cdot cm^2$, depending on operating conditions such as temperature and hydration. The water uptake of the membrane is moderate, typically below 25 %, which supports membrane hydration and conductivity without excessive swelling or mechanical distortion.

Due to its relatively low thickness, the FAS-50 provides a favourable balance between ionic conductivity and mechanical integrity, contributing to low ohmic losses during operation. In the experimental tests, this membrane enabled the achievement of current densities up to 1.8

$A \cdot cm^{-2}$ at approximately 2.0 V, demonstrating performance within the expected range for high-efficiency AEM water electrolysers.

3.2 Methods

3.2.1 Experimental Setup

Different setups were used for different purposes. The initial setup provided from NET4CO2 were mainly to characterise and test the ink itself where the second setup used at CEFT/FEUP had the purpose of testing the most promising in-house inks under real life conditions.

3.2.1.1 Batch-type cell

In this project, a 2-C BM FC EC 50 mL electrochemical cell from Redox.me is employed to perform front-contact electrochemical measurements on flat electrodes. The configuration used includes a 15×15 mm^2 working electrode, corresponding to a nominal exposed area of 1.33 cm^2. The total internal volume of the cell is 50 mL, with a functional electrolyte volume of approximately 45 mL in the working compartment. This two-compartment design incorporates a nanoporous alumina frit with 2 mm thickness to separate the counter electrode chamber, minimizing contamination and ensuring a stable ionic pathway. The cell body is constructed from chemically inert materials such as borosilicate glass and PEEK, allowing compatibility with both aqueous and organic media. The bottom-mount system provides secure and reproducible electrode placement, while the top compartment accommodates standard reference and counter electrodes. Dedicated ports for gas purging and electrolyte management further enhance the control over experimental conditions, making this cell particularly suited for detailed electrochemical characterisation of catalytic surfaces.

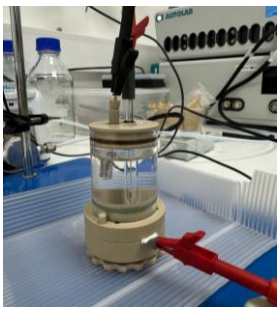

Figure 6 - Experimental setup for the batch-type cell tests at NET4CO2

3.2.1.2 AEM Electrolyser

The single-cell electrolyser used in this study was custom-assembled and specifically designed to allow comparative evaluation of membrane and electrode materials under controlled

conditions. The cell featured an active geometric area of 5 cm^2, and was configured for double-feed operation, meaning that the electrolyte solution 1 M KOH was supplied simultaneously to both the anode and cathode compartments. This configuration ensured symmetrical hydration and minimised concentration gradients.

The end-plates were fabricated from stainless steel 316L with overall dimensions of 8 × 8 × 2 cm^3, providing mechanical rigidity and chemical resistance in the alkaline environment. Between the end-plates, titanium bipolar plates were installed, featuring a single serpentine flow field. This design ensured uniform distribution of the electrolyte across the active area while maintaining low pressure drop and good gas-liquid transport. Titanium was selected due to its excellent corrosion resistance under anodic polarisation and compatibility with long-term alkaline operation.

Gaskets made of PTFE, also known as Teflon were used to ensure sealing and mechanical spacing. Their thicknesses were tailored to match the electrode type used, with common values of 0.55 mm for the anode when using the electrode and 0.25 mm for the cathode. In cases involving in-house prepared electrodes, the anode gasket was adjusted to 0.21 mm to match the reduced thickness of the gas diffusion layer (GDL). This careful adjustment ensured uniform compression across the membrane-electrode assembly, minimizing contact resistance and ensuring stable electrochemical behaviour.

The electrolyser cell assembly sequence included alternating layers of gaskets, electrodes, membrane, and bipolar plate, using stainless steel alignment pins and torque-controlled bolts tightened progressively to 3.0 Nm in a crisscross pattern to ensure mechanical integrity and reproducibility between tests. The modular and reconfigurable nature of the setup allowed for systematic substitution of membranes and electrodes during the experimental campaign.

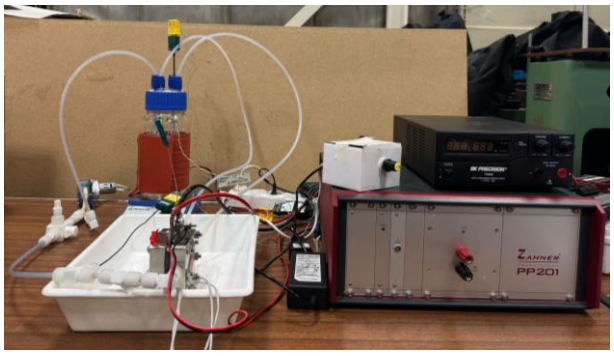

Figure 7 - Experimental setup of the AEM electrolyser at CEFT/FEUP

3.2.2 Deposition Techniques

As mentioned previously, the in-house catalytic inks were deposited onto the substrates using, an airbrushing technique with a DEXTER DX-1839 airbrush. During the deposition process, the

substrate was positioned on a hot plate that was maintained at a temperature of 60°C. This elevated temperature was intended to facilitate the rapid evaporation of the solvent and ensure the formation of a uniform film.

The inks were applied in multiple passes to achieve the desired catalyst loading. After the deposition process, the electrodes were allowed to dry at ambient temperature for a period of 24 hours prior to being weighed. This step enabled the determination of the final catalyst mass.

3.2.3 Characterisation Techniques

There are several techniques available for the characterisation of electrochemical processes, including chronoamperometry (CA), chronopotentiometry (CP), cyclic voltammetry (CV), and electrochemical impedance spectroscopy (EIS), among others. However, this section will focus only on the techniques that were specifically employed in the experiments of this work.

3.2.3.1 Chronopotentiometry

Chronopotentiometry is a technique in which a constant current is applied to an electrochemical system while the resulting potential is recorded over time. It serves as a valuable tool for evaluating the durability and potential stability of electrode materials under fixed current operation, closely simulating practical electrolysis conditions. Thus, in this work the results were provided through polarisation curves.

Polarisation curves are fundamental tools for evaluating electrochemical performance of an AEM electrolyser. These curves plot the electrolyser voltage against current density, revealing key contributions from kinetic, ohmic, and mass transport losses. In flow-cell configurations, enhanced mass transfer and uniform reactant distribution often lead to improved performance, reflected in lower overpotentials at given current densities. Importantly, comparing polarisation curves obtained under identical conditions is a powerful method for benchmarking different catalysts, as it allows for the direct assessment of their electrocatalytic activity, efficiency, and stability. Such comparisons are essential in identifying the most promising materials for scale-up and practical application in continuous electrochemical systems.

The performance of selected in-house anodes developed at NET4CO2 were evaluated in an AEM electrolyser at CEFT. The single-cell electrolyser was integrated into a custom-built bench-scale test station, consisting of a feed tank, peristaltic pump NE-900B, DC power supply BK Precision 1900B, heating system, and data acquisition software operated through LabVIEW.

The electrolyte 1M KOH was preheated in the feed tank to the target temperature at the electrolyser inlet (60 °C for most tests) using an electrically controlled heater pad governed by real-time readings from type-K thermocouples located at the tank, inlet, and outlet. The

heated electrolyte was pumped into the cell at a constant flowrate of 110 Ml·min^{-1}, with flow directed simultaneously to the anode and cathode compartments.

For each test, a membrane activation step was carried out by applying a current sufficient to bring the cell voltage close to 2.5 V, followed by a stabilisation phase at ~2.0 V for 2 hours.

In the final stage, polarisation curves (i vs V) were generated using a stepwise current ramp from 0 to 0.1 A·cm^{-2} with increments of 0.02 A·cm^{-2}, and above 0.1 A·cm^{-2} with increments of 0.10 A·cm^{-2}.

Each step was maintained for 1 minute, and the voltage was recorded at the end of the period. A cut-off voltage of 2.0 V was applied to prevent cell degradation. Further analysis and comparison of the I-V curves were performed to find the most promising catalysts.

3.2.3.2 Cyclic Voltammetry (CV)

Cyclic voltammetry (CV) is a fundamental technique in electrochemical analysis, widely employed to investigate redox processes, surface properties, and the capacitive behaviour of electrode materials. Its capacity to provide insight into both Faradaic and non-Faradaic processes, as well as its ability to elucidate kinetic and mass transfer phenomena, makes it indispensable in the development of advanced electrocatalysts.

In a typical CV experiment, the potential of a working electrode is swept linearly back and forth within a defined voltage window while the resulting current is recorded. The shape and symmetry of the resulting voltammogram allow for the identification of electrochemical signatures associated with specific redox transitions, capacitive contributions, adsorption phenomena, or diffusion limitations. Notably, changes in peak position, peak current, and hysteresis provide essential information on the reversibility of electrochemical reactions, electroactive surface area, and stability of the electrocatalyst under operating conditions [40, 41].

The technique is particularly useful in distinguishing between surface-controlled and diffusion-limited processes. Through systematic variation of the scan rate and subsequent i vs υ or i vs $\upsilon^{1/2}$ analysis, one can infer the dominant mechanism governing the electrode response—a powerful diagnostic for evaluating catalyst performance before scale-up.

In the present work, CV is used as a rapid screening method to assess and compare the performance of the different in-house synthesised catalytic inks previously mentioned. These inks were first tested in the batch cell to evaluate their electrochemical behaviour and stability under specific conditions. The tests were conducted in 1 M KOH using the three-electrode configuration described earlier in this section as the first voltammogram being evaluated using a common scan rate of 50 mV s^{-1} in a total of 5 scans. After obtaining the first voltammogram,

the scan rates were varied from 100, 75, 50, 25 and 10 mV s^{-1} for about 5 to 10 scans depending on the stability of the results. Two types of scan rate tests were made: one in the Faradaic zone where is possible to evaluate the behaviour of the redox probe of the nickel species, and the other in the capacitive zone where no Faradaic reaction occurs. Figure 8 unveils the analysis of a voltammogram.

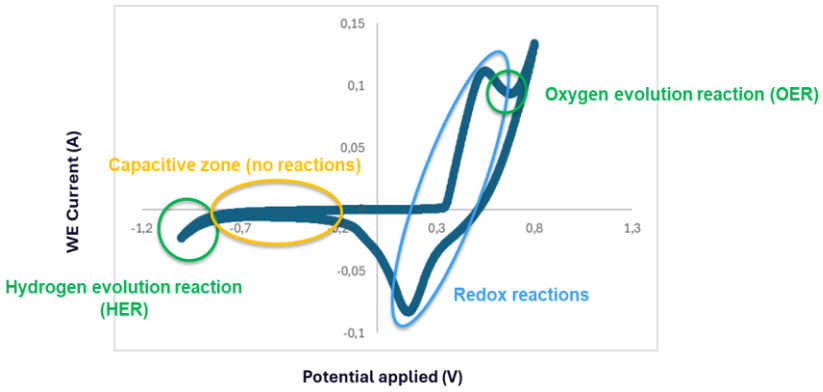

Figure 8 - Voltammogram with the respective identified zones from a three electrode configuration using a nickel based catalytic ink

As a result, voltammograms provide immediate information on key characteristics such as onset potential for the oxygen evolution reaction (OER), double-layer capacitance, and presence of redox-active species.

This pre-evaluation step is crucial in narrowing down the most promising ink formulations for subsequent testing in AEM electrolyser. While batch systems offer controlled environments ideal for exploratory studies, they inherently lack the convective and continuous features of typical electrolysers, where reactants are constantly fed and products removed. Flow systems often show enhanced mass transport, reduced concentration gradients, and better scalability, making them more representative of real electrochemical reactors. Therefore, only the inks that demonstrate stable and reproducible CV profiles in the batch setup were then tested in the electrolyser system.

Furthermore, CV is also leveraged as a quality control tool to detect potential contaminants that may affect the reliability of the electrochemical results. For instance, trace Fe impurities in KOH electrolytes can substantially alter the OER activity of Ni-based electrodes. Conditioning experiments involving thousands of CV cycles have shown the incorporation of Fe into the electrode matrix, significantly boosting apparent activity and complicating data interpretation. As such, CV becomes instrumental not only in performance evaluation but also in ensuring the chemical integrity of the system [42].

By integrating CV as a preliminary step in the experimental pipeline, this project ensures a rigorous and informed transition from lab-scale batch evaluations to more dynamic flow-cell electrolyser testing. This strategic approach enhances the reliability of material selection and contributes to the overall development of sustainable and scalable electrocatalytic systems.

To assess the electrochemical performance of the batch-type cell, two key indicators were considered: the capacitive current, which reflects the electrode's double-layer charging behaviour, and the reversibility of the redox probe, which provides insights into the electron transfer kinetics and diffusion characteristics of the system.

-Capacitive Current

When a voltage ramp is applied to an electrode in the absence of faradaic processes, a steady capacitive current, i_c, arises due to the charging of the electrical double layer. This phenomenon results from the displacement of ions at the electrode/electrolyte interface. The capacitive current exhibits a linear dependence on the scan rate, υ, and can be expressed as equation 4 [27]:

$$i_c = C_{DL} \cdot \upsilon \quad (4)$$

where i_c is in ampere (A), C_{DL} is the double layer capacitance in Faraday (F) and υ is the scan rate (V s-1).

-Reversibility of the redox probe

In an electrochemically reversible system, the oxidation and reduction processes are both kinetically fast and occur without significant structural reorganisation of the redox species. This enables the redox couple to maintain equilibrium at the electrode surface throughout the potential scan. Such behaviour manifests in CV as a symmetric pair of anodic and cathodic peaks, characterised by a peak-to-peak separation (ΔEp) of approximately 59 mV at 25 °C for a one-electron process, as predicted by the Nernst equation and the Randles–Ševčík model under semi-infinite linear diffusion conditions.

Quantitatively, the reversibility of the redox probe is evaluated by several key criteria:

a) Peak Potential Separation (ΔEp): For a fully reversible one-electron process, ΔEp ≈ 59 mV at slow scan rates (e.g., 50–100 mV s^{-1}). An increase in ΔEp at higher scan rates may indicate kinetic limitations or ohmic drop.

b) Peak Current Ratio (I_{pa}/I_{pc}): In a reversible system, the ratio of anodic (I_{pa}) to cathodic (I_{pc}) peak currents approaches unity, indicating equal forward and reverse current magnitudes.

c) Linear Dependence of Peak Current on √Scan Rate: For diffusion-controlled processes, the peak current (I_p) scales linearly with the square root of the scan rate ($\upsilon^{1/2}$), in agreement with the Randles–Ševčík equation [43].

3.2.3.3 Dynamic light scattering (DLS)

Dynamic Light Scattering (DLS) is a laser-based technique that analyzes Brownian motion (the random movement of particles suspended in a fluid due to collisions with the fluid´s molecules) of particles suspended in a liquid to determine their hydrodynamic diameter and size distribution relying on intensity fluctuations of scattered light. In the field of inks and pigment formulations, DLS plays a crucial role by monitoring the dispersion´s quality, detecting aggregation or coalescence that may lead to nozzle clogging or uneven color output, and ensuring colloidal stability throughout development.

In this work, DLS was employed specifically to characterise the catalytic inks developed by measuring the nanoparticles' size distribution, assessing polydispersity, and identifying any early signs of aggregation and new compounds. This ensures that the inks maintain uniform and stable dispersions that are critical for achieving consistent electrode coatings, optimal catalytic activity, and reproducible electrochemical performance.

3.2.3.4 X-ray diffraction (XRD)

While DLS was used for the ink characterisation, X-ray Diffraction (XRD) was followed and used to characterise its deposition in the substrate. XRD is a powerful analytical technique used to probe the crystallographic structure of materials by measuring the angles and intensities of X-rays diffracted from atomic planes within a sample. In thin-film or coated systems, it also helps identify the presence of specific crystalline phases or unwanted impurities, detect stress or strain in the deposited film, and estimate crystallite size.

The main purpose of XRD in this work was to validate the ink deposition by confirming that the intended crystalline phases have been successfully applied to the substrate, that their structure matches the desired expectations, and confirm the absence of undesired byproducts or impurities. This validation step is crucial to ensuring reproducible, high-performance electrode coatings and reliable electrochemical behaviour.

4 Results and discussion

In this section, the most significant findings on electrochemical behaviour and product assessment are presented. Each assay includes at least one consistent replicate, and further experimental details are available in Annex A.

4.1 Electrodes developed

The electrodes were developed at NET4CO2 following the procedure explained in the previous section. The developed electrodes after electrochemical tests can be observed in table 2 with their respective compositions.

Table 2 - In-house electrodes prepared at NET4CO2

Formulation	1	2	3	4
Ink composition (% Nickel)	100 %	95 %	90 %	85 %
Electrode	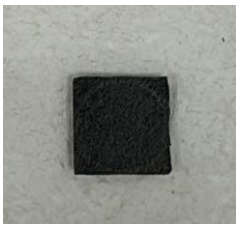	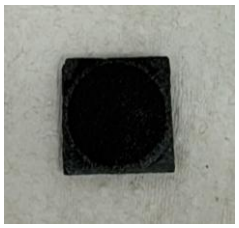	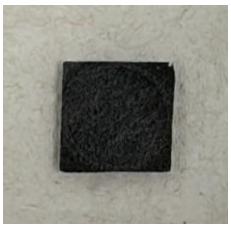	

Beyond these formulations, there was still the development of another two electrodes such as the commercial $NiFe_2O_4$ and Ni/SiO_2-Al_2O_3 that are important for our results whether as term of comparison or as promising alternative.

4.1.1 Dynamic light scattering (DLS)

For the dynamic light scattering tests there were some fluctuations that compromised the results since this type of testing can only be done on dispersions and not solutions and our formulations had such low quantities of nickel (II) nitrate hexahydrated and copper (I) oxide. Thus, it was not possible to obtain the results for the 100 % nickel ink, nickel dissolved in the solvent making the system control program consider it as a solution and not being able to test. For the 90 % nickel, the remaining quantity that was going to be used in these tests was not enough to be able to get results. Finally, for the 95 % and 85 %, enough amounts of ink were available for testing. For each DLS measurement, two key parameters were monitored to ensure data quality: obscuration and PIDS (Polarisation Intensity Differential Scattering). Obscuration reflects the proportion of laser light blocked by particles in the dispersion, while the PIDS percentage indicates the quality of the scattering signal based on polarisation differences, with optimal values around 45 % for accurate particle size determination. However, when testing

these formulations, the compositions yielded PIDS values of only 18 % which falls below the ideal threshold. As a result, the measurements were less accurate, but it was still possible to obtain them. The results are presented in Annex A.1.

4.1.2 X-Ray diffraction (XRD)

For the XRD analysis, only the ink containing nickel supported on silica/alumina was tested. Given that all inks were deposited using the same procedure and under identical conditions, it was assumed that the structural characteristics observed for this representative sample would be consistent across the remaining formulations. As such, the results obtained from the nickel/silica–alumina ink were used to validate the effectiveness and reproducibility of the deposition method applied to all developed inks. Along with the DLS results, in Annex A.1 there is a graphical representation of these results.

4.2 Electrochemical tests - Batch cell

As mentioned before, the initial stage of this work started in the electrochemical batch cell and performing cyclic voltammetry analysis. This allowed to characterise each ink before using it in the AEM electrolyser and compare it with the commercial catalyst $NiFe_2O_4$. Three main parameters were focused on during these analyses: Double layer capacitance, electron transfer and most importantly, on-set voltage.

In the beginning, a baseline analysis was carried out just using the carbon paper without any catalyst addition. In figure 9, the cyclic voltammetry resulted from the baseline analysis can be observed.

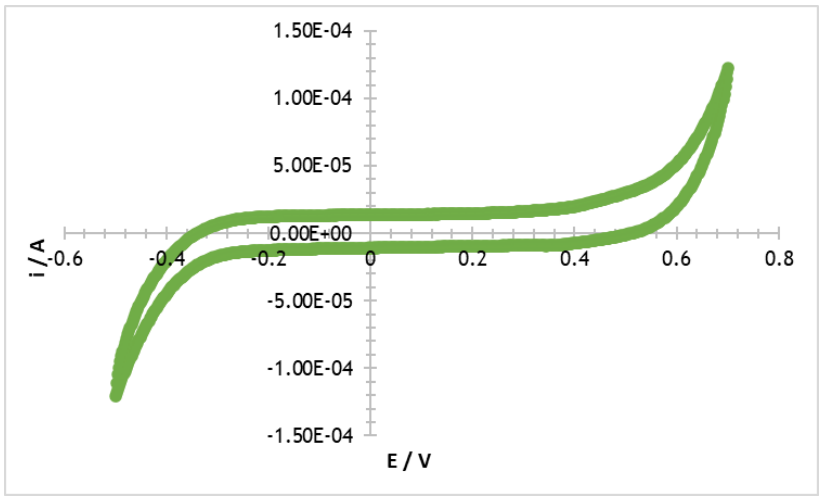

Figure 9 - Cyclic voltammetry at 50 mV s^{-1} for carbon paper electrodes without catalyst vs Ag/AgCl.

The cyclic voltammogram presented above illustrates the electrochemical behaviour of planar carbon paper in 1 M KOH. The potential range investigated spans from −0.6 V to +0.7 V vs Ag/AgCl to encompass the regions where the hydrogen evolution reaction (HER) and oxygen evolution reaction (OER) start to occur.

Throughout the central portion of the scan, approximately between −0.2 V and +0.4 V, the current remains relatively constant and close to zero, indicating the absence of significant faradaic processes. This behaviour is characteristic of electric double-layer charging and confirms the electrochemical inertness of the naked carbon surface within this window.

At more negative potentials, a marked increase in cathodic current is observed beginning around −0.4 V, suggesting the onset of HER. Conversely, in the anodic direction, the current rises sharply beyond +0.6 V, which is indicative of the onset of OER.

The overall shape of the voltammogram is nearly symmetric with low hysteresis between the forward and reverse scans, further supporting the dominance of capacitive behaviour and the absence of any significant redox activity.

4.2.1 Double layer capacitance

The double-layer capacitance can be experimentally determined using cyclic voltammetry by analysing the capacitive current response in a non-Faradaic potential region, a window in which no redox reactions occur. So, after doing the voltammograms, the voltage range was chosen where the current response is flat and featureless. This range was then used to perform a series of CV scans at different decreasing scan rates from 100 to 10 mV s^{-1} to avoid the overvoltage the electrode and damage it. In Figure 10 the results from the scan rates are represented.

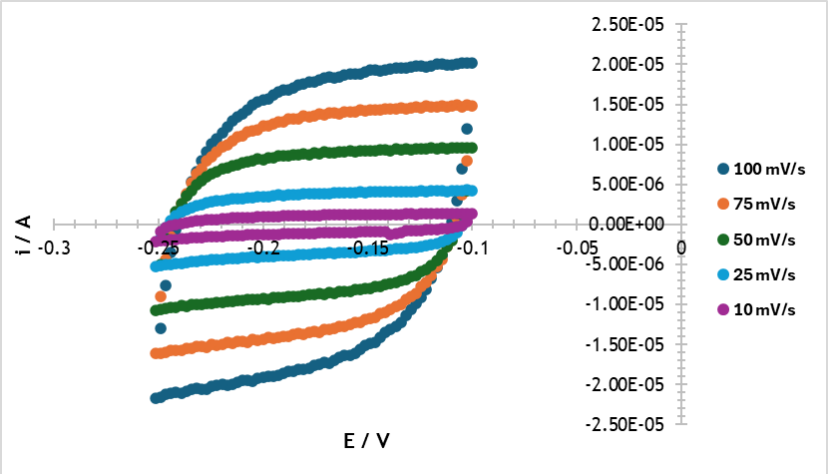

Figure 10 - Scan rate results at the capacitive (non-Faradaic) zone of the voltammogram corresponding to the planar Toray carbon paper

For each scan rate, the anodic and cathodic currents were recorded at the midpoint of the selected potential window, so the capacitive current i_c was determined by calculating the average of the absolute values of these two currents, as follows:

$$i_c = \frac{|i_{anodic}| + |i_{cathodic}|}{2} \quad (5)$$

The parameters obtained for the plane carbon paper are presented in table 3.

Table 3 - Resulting parameters for the double layer capacitance calculation

υ (V s^{-1})	V	i anodic (A)	i cathodic (A)	ic
0.1	-0.176	1.78E-05	-1.76E-05	**1.77E-05**
0.075	-0.176	1.36E-05	-1.34E-05	**1.35E-05**
0.05	-0.176	8.95E-06	-8.80E-06	**8.87E-06**
0.025	-0.176	3.84E-06	-3.68E-06	**3.76E-06**

The resulting values of i_c were then plotted as a function of the scan rate υ, yielding a linear relationship from which the slope corresponds directly to the double-layer capacitance [27], as can be observed in Figure 11.

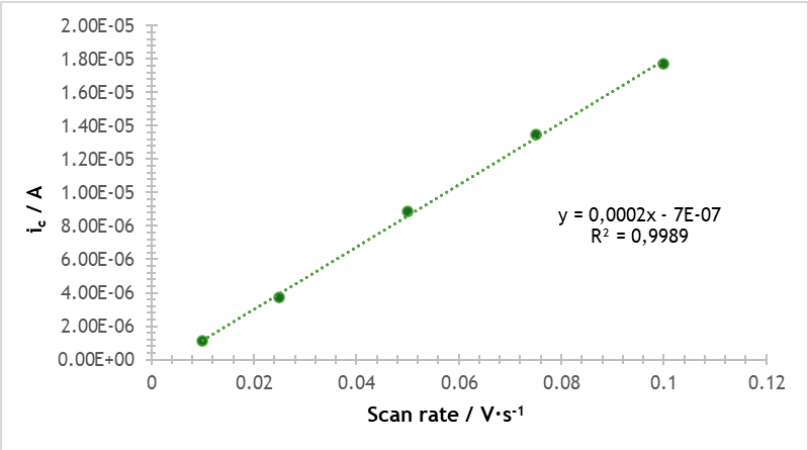

Figure 11 - Double-layer capacitance results

The obtained value of $2 \cdot 10^{-4}$ Farads (F) is the term of comparison for the double layers capacitances analysis of the different catalytic inks.

4.2.2 Catalytic inks

After the baseline is determined, the developed catalytic inks were tested. As mentioned previously, the first ink tested was the nickel-based ink supported on silica/alumina from Merck, which showed irregular and inconsistent behaviour during testing as can be observed in figure 12.

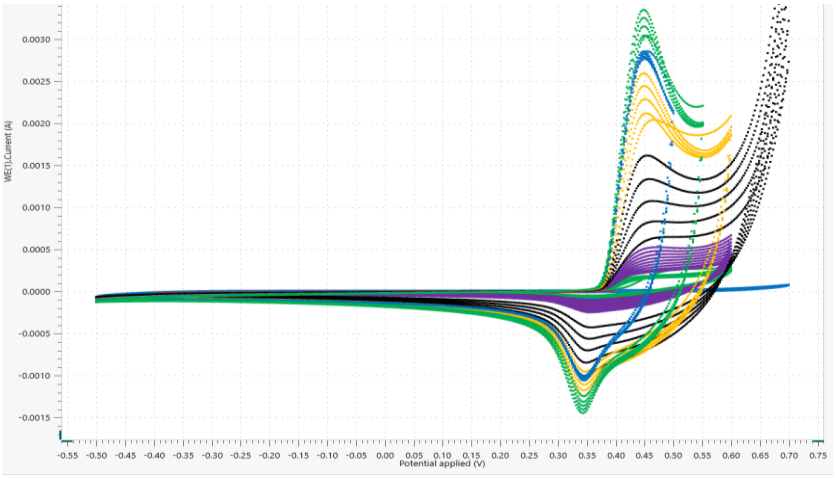

Figure 12 - Voltammograms for carbon paper electrodes with nickel-based supported on silica/alumina with approximately 65 wt.% metal loading

Due to this factor, the tests were excluded from the pre-evaluation analysis. However, in order to document the procedure and ensure transparency, the only available way to include the results was through a printout of the original graphs. These are presented solely for illustrative purposes and are not considered in the interpretation or conclusions of the work.

The test proceeded with a new set of inks formulated using Nickel(II) nitrate hexahydrate as the main precursor, without and with increasing additions of Copper(I) oxide. These new formulations were tested following the same procedure previously described for the baseline determination. In Figure 13 the voltammograms for the pure Nickel(II) nitrate hexahydrate are represented.

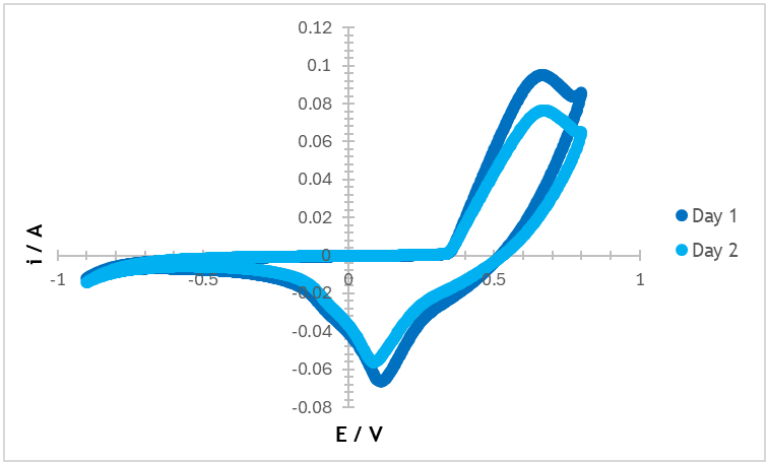

Figure 13 - Voltammograms obtained for the electrodes loaded with 100 % Nickel(II) nitrate hexahydrate deposited

A comparison of this voltammogram with that of the unmodified planar carbon paper reveals a substantial shift in electrochemical behaviour. While the bare carbon paper exhibited a largely capacitive response with minimal faradaic features, the electrode modified with 100 % Nickel(II) nitrate hexahydrate displayed well-defined redox peaks and a pronounced increase in current density.

The occurrence of these redox peaks is indicative of the reversible transformation between Ni(II) and Ni(III) species at the electrode surface. Specifically, the cathodic peak observed from −0.2 A to −0.6 A is associated with the reduction of Ni(III) into Ni(II), while the anodic peak between approximately 0.4 V and 0.6 V reflects the oxidation of Ni(II) to Ni(III). These transitions enable the surface to enter catalytically favourable oxidation states, specifically NiOOH.

These $Ni(OH)_2$/NiOOH transitions serve as vital precursors to OER, acting as mediating steps that both store and transfer oxidative equivalents. Therefore, their presence validates the effectiveness of the ink formulation in enhancing OER activity and demonstrates that the electrode is not simply an inert support but an electroactive catalyst [44].

The OER is characterised by a sharp increase in current beyond 0.6 V.

Following the same procedure, next step is the determination of the double layer capacitance. In Figure 14 the results from the scan rates for the pure Nickel(II) nitrate hexahydrate are represented.

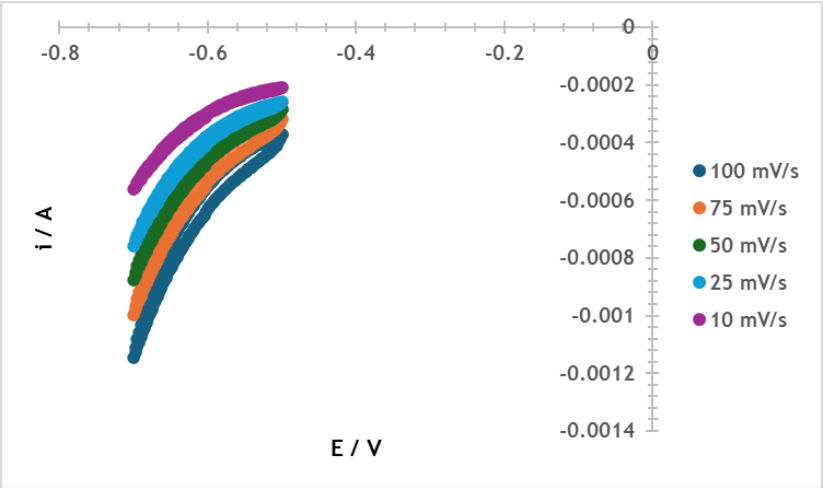

Figure 14 - Scan rate results at the capacitive (non-Faradaic) zone of the voltammogram for the electrodes loaded with 100 % Nickel(II) nitrate hexahydrate deposited

The results are not the ones meant to be expected. The profiles obtained are very different from the ones for the planar carbon paper. In the context of the present system, the double-layer region cannot be regarded as ideally capacitive, thereby invalidating the simple linear model. Real electrodes (particularly those with porous structures or modifications to nickel) demonstrate suboptimal charge storage behaviour due to factors such as surface roughness, heterogeneity, ion diffusion within pores, and pseudocapacitive redox contributions. Instead of behaving like a pure capacitor, these systems follow a constant phase element (CPE) model, which displays scan-rate-dependent current and a frequency-dependent phase response, thereby invalidating the direct extraction of true double-layer capacitance from CV slopes [45].

Consequently, any capacitance derived from CV in such systems should be regarded as apparent, and rigorous determination requires impedance spectroscopy with CPE-based equivalent circuits.

On contrary to the planar carbon paper electrodes, there were redox reactions occurring in its surface. Hereupon it is possible to study the behaviour of these reactions and the type of control that is in command by doing the scan rate tests in the Faradic zone. In Figure 15 these results are represented.

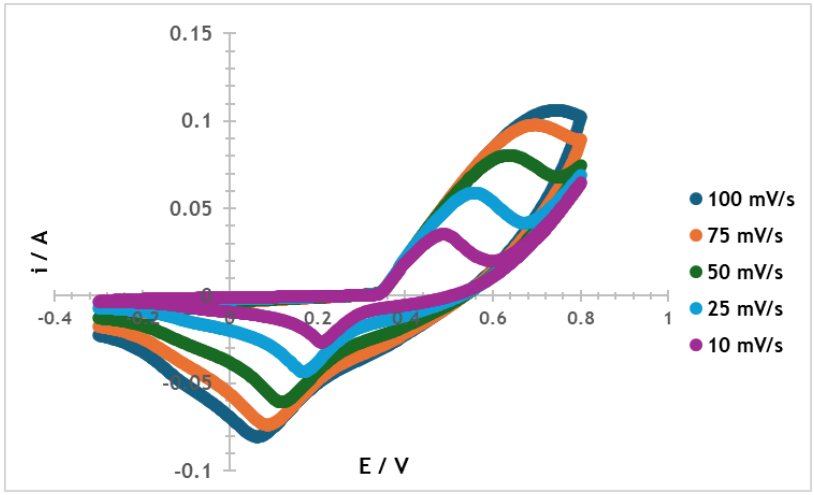

Figure 15 - Scan rate results at the Faradaic zone of the voltammogram for the electrodes loaded with 100 % Nickel(II) nitrate hexahydrate deposited

In Figure 16, the complementary results for linearization and the oxidation-reduction behaviour are represented.

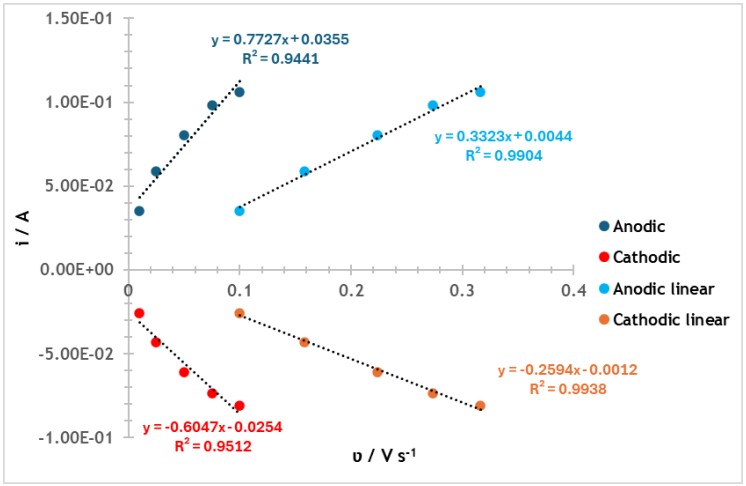

Figure 16 - Linearization of the i vs υ plots for the electrodes loaded with 100 % Nickel(II) nitrate hexahydrate deposited

When plotting the peak currents against the square root of the scan rate, the resulting graph exhibits excellent linearity with minimal interceptions. According to the Randles-Ševčík equation, this proportional relationship is a classic hallmark of a diffusion-controlled and electrochemically quasi-reversible redox process. In these cases, the reactants reach the electrode surface primarily through diffusion, and the electron-transfer kinetics are fast compared to mass transport.

The results give R^2 above 0.99 for both anodic and cathodic peaks confirming this behaviour. Furthermore, near-zero intercepts suggest that the currents are dominated by faradaic response rather than background charging. Therefore, we can confidently conclude that the observed Ni(II)-Ni(III) redox transitions are diffusion-limited and quasi-reversible, validating the use of the Randles–Ševčík model.

Following the same steps, the remaining formulations are then tested. Their voltammograms and respective scan rate tests for each zone are presented in Annex A.2. As expected, since it is used the same nickel but with increasing percentages of copper oxide (II), we couldn´t calculate the double layer capacitance because all of them gave a similar profile to the 100 % one. On top of that, when plotting the peak current vs scan rates in the Faradaic zone there is a better linearization when the scan rates were changed to their square roots validating again the Randles–Ševčík model and confirming the domination of diffusion-controlled reactions.

Besides doing all this tests to characterise our formulations, the most important value for the pre-tests before actually using them in a AEM electrolyser is the actual potential onset (and it´s stability of course) obtained from the initial voltammogram. The potential onset is the minimum value of potential needed to start the oxygen evolution reactions so, the lower this value, the better.

Keeping in mind all these parameters for our formulations, the overall results for each tested ink are presented in table 4.

Table 4 - Overall results from the ink characterisation

Ink Composition (% Nickel)	CDL (Double Layer Capacitance)	Ni Oxidation Behaviour (Randles-Sevcik model)	OER Promotion (Average Onset Potential)
100	Unexpected behaviour making not possible to obtain this value	Diffusion-controlled	0.79 V
95			1.00 V
90			0.77 V
85			0.80 V

Every ink gave similar results in the characterisation part. However, for the OER promotion the onset potential varies without any similarity. The worst result obtained was for the 95 % nitrate nickel hexahydrate and 5 % copper oxide with the value of 1.09 V. Although it is not possible to confirm why this value deviates so much from the others, the thinking behind this is probably a bad deposition of the ink, a non-optimal distance between the reference and working

electrode in the batch cell or maybe the ink is just not ideal. The remaining samples gave values close to each other becoming promising for future testing in the AEM electrolyser.

The experimental procedure of the AEM electrolyser tests is clarified in annex A.5 along with its assembly in annex A.4.

4.3 Electrochemical tests in the AEM electrolyser

For the final stage of testing, we now get to use the AEM electrolyser and plot the polarisation curve. It is important to note that for these tests the ink was deposited on a 2.23 x 2.23 cm stainless steel electrode following the same deposition method as when testing with the batch cell.

With the aim of doing a benchmark analysis, a commercial NiFe2O4 ink tested and produced at CEFT/FEUP and tested at the same operating conditions. For fair comparison, the substrate material and the kind of membrane were the same as the used for the developed catalytic inks.

In Figure 17, the validation of the deposition method and respective polarisation curves are represented.

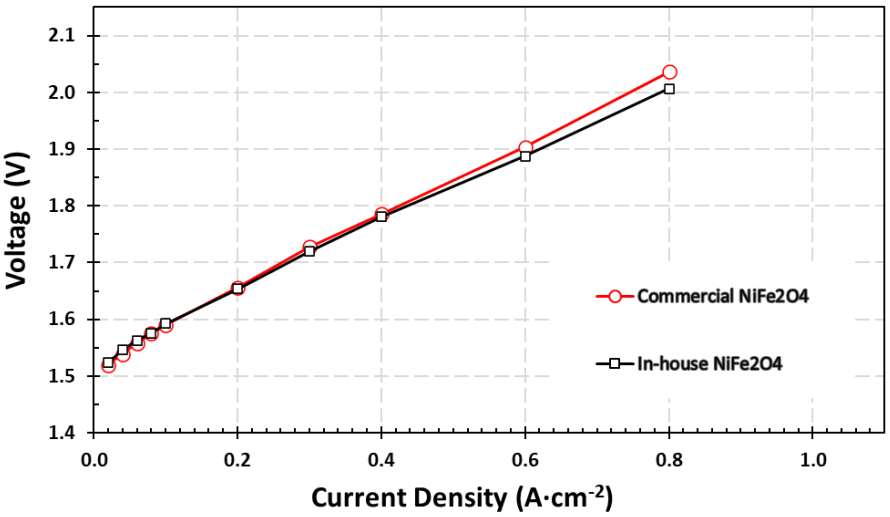

Figure 17 - I-V polarisation curves for the commercial and in-house commercial NiFe2O4 electrode

For a more reliable analysis, a polarisation curve was plotted using a gas diffusion electrode (GDE) prepared with a commercial $NiFe_2O_4$ catalyst. This result was then compared with a reference polarisation curve acquired at CEFT/FEUP using the same commercial NiFe2O4 material. The objective of this comparison was twofold: first, to verify the consistency between

both results, and second, to assess whether the newly obtained curve could be considered representative for further analysis.

The observed similarity between the two polarisation curves confirmed the validity of the data, thereby enabling the application of the new curve as a benchmark in subsequent evaluations.

The results were obtained using the program LabVIEW. For a better discussion of the effects of the electrodes and the membrane, the polarisation curves can be evaluated in two regions: the activation region that is represented by the voltage values for current densities up to 0.1 A·cm-2 and the ohmic region being slope of the curves for current densities above 0.1 A·cm-2. For all the tests, the pressure, feed concentration and feed flowrate were kept constant at 1 atm (absolute), 1 M KOH and 110 mL·min-1, respectively.

At low current densities, characteristic of the activation region is dominated by the kinetic limitations of the electrochemical reactions OER and HER. The relatively low starting voltage of around 1.51-1.52 V indicates that the $NiFe_2O_4$ catalyst provides sufficient catalytic activity to initiate the reaction with modest activation losses, especially considering that it is a non-noble material. Although it is not as active as Ir-based catalysts, this performance is still promising, given the abundance and cost-effectiveness of the material.

As the current density surpasses 0.1 $A \cdot cm^{-2}$, the curve shifts to a nearly linear region, indicating the predominance of ohmic losses within the cell. In this regime, the slope of the polarisation curve reflects the system's internal resistance, including contributions from the membrane, electrodes, and electrical contacts. The linearity of this region indicates that the system is well-constructed with stable pathways for ion and electron transport. At a current density of 0.6 A cm^{-2}, the cell voltage reaches approximately 1.90 V and continues to rise steadily toward 2.0 V at about 0.85 A cm^{-2}. These results demonstrated values that are remarkably like those typically reported for iridium-based catalysts under equivalent conditions. Specifically, the operating voltages observed across the full range of current densities fall within the expected envelope for Ir-based anodes, thereby confirming that NiFe2O4 offers a competitive alternative despite its non-noble composition and it´s suitability as a commercial reference material. The comparative polarisation curve between $NiFe_2O_4$ and Ir is presented in Annex A.3.

After the baseline was provided it was time to test out the in-house inks and compare them with the commercial. These results are represented in Figure 18.

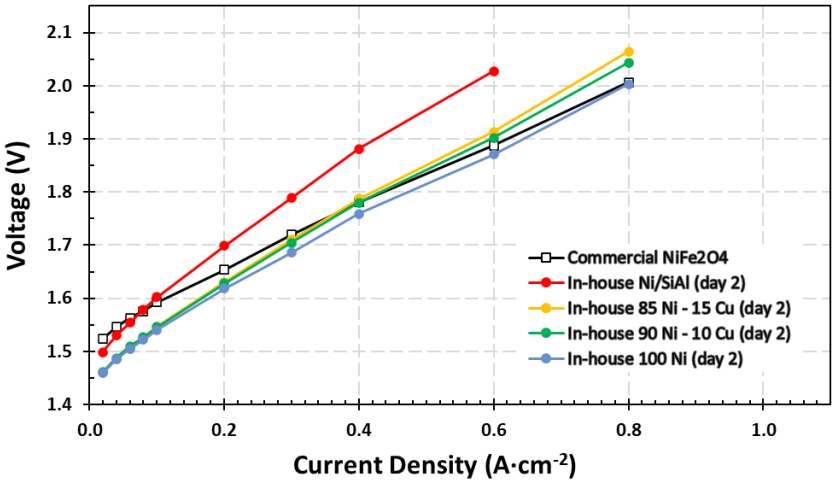

Figure 18 - Polarisation curves for every ink formulated

Pure nickel demonstrated the lowest operating voltage among the inks that were examined, suggesting its potential for enhanced catalytic activity in the water-splitting process within 1 M KOH. This assertion is corroborated by the results of polarisation curves, which demonstrate that the 100 % Ni ink sample attained lower cell voltages. In contrast, the 90 % Ni – 10 % Cu and 85 % Ni – 15 % Cu inks exhibited higher voltages at high currents when compared with 100 % Ni, with an incremental loss of performance as copper content was added. Conversely, the Ni/SiAl ink exhibited the highest voltages, thereby demonstrating its worst performance among the inks tested.

According to extant literature, the addition of copper has been demonstrated to enhance performance in mixed Ni-Cu systems under certain conditions. However, this enhancement is contingent upon the optimisation of composition and phase structure. Conversely, in the context of simple Ni-Cu oxide inks, an increase in Cu appears to engender a reduction in conductivity and a concomitant introduction of less active oxide phases, thereby elevating the overpotential [46].

Nickel has been observed to readily form a surface layer of $Ni(OH)_2$/NiOOH in alkaline environments. These species play a pivotal role in both OER and HER, facilitating rapid proton-coupled electron transfer (PCET) and exhibiting favourable Tafel slopes. Metallic nickel exhibits high conductivity beneath such layers, thereby maintaining low charge-transfer resistance [47].

In opposition, the introduction of copper results in the formation of Ni-Cu oxide structures that frequently exhibit reduced conductivity and diminished capacity to generate catalytically active hydroxide phases. Although there are improvements in the activation region, the research had demonstrated that while the incorporation of low levels of copper (e.g., 5 %) can enhance oxygen evolution reactions (OER) in Ni-Cu catalysts, the presence of excessive copper results in increased overpotentials at higher currents and diminished kinetics.

The progression from 10 % to 15 % Cu illustrates this degradation since 90 % Ni – 10 % Cu exhibits a minor performance drop, and 85 % Ni – 15 % Cu drops further, lagging pure Ni.

5 Conclusion

The goal of this study was to develop and evaluate alternative catalytic materials for the oxygen evolution reaction (OER) to enhance the sustainability and cost-effectiveness of water and CO_2 electrolysis systems which are crucial for the development of eFuels. In this sense, different anode formulations were identified focusing on specific features: low-cost, scalable, environmentally friendly, and made from earth-abundant metals to avoid the limitations associated with noble metal catalysts, such as iridium oxide IrO_2.

A screening strategy was employed, beginning with batch-type electrochemical tests to characterise the redox activity, double-layer capacitance, and onset potential of different in-house formulated catalytic inks. As a result, 100 % nickel(II) nitrate hexahydrate-based ink exhibited the most promising electrochemical behaviour. This included clear redox transitions associated with Ni(II)/Ni(III), favourable onset potential, and strong diffusion-controlled characteristics. These characteristics were confirmed by Randles–Ševčík analysis. Other compositions, where copper oxide was added (5–15 %), exhibited progressively lower performance.

After the batch electrochemical tests, the most promising catalytic inks were tested under more realistic conditions as described previously using a custom-built AEM electrolyser. Polarisation curves confirmed that pure nickel-based ink outperformed all other in-house formulations by achieving the lowest cell voltages across a range of current densities. Comparing with the commercial material $NiFe_2O_4$, the in-house Ni-based ink showed comparable performance, and in some cases superior performance like the 100 % nickel ink, despite its simpler composition and synthesis process.

In a nutshell, the outcomes demonstrate the viability of formulating sustainable anodes without use of noble metals or intricate synthesis methodologies. The preparation method, which is based on airbrushed ink deposition and mild thermal treatment, offers a practical and scalable route for catalyst application. This method requires no hazardous solvents or sophisticated equipment. This initiative aligns with the project's fundamental vision of promoting accessible green technologies, thereby reducing environmental and economic barriers.

The identification and evaluation of low-cost, earth-abundant materials that demonstrate promising electrochemical performance in alkaline environments are the main output of this research. Finally, this work opens a new window for sustainable electrolyser solutions contributing to the development of feasible electrochemical technologies that support decarbonisation strategies.

6 Assessment of the work done

6.1 Objectives Achieved

The objective of this project was to develop and characterise sustainable anodes for the OER process. The main driver was to privilege the use of cost-effective abundant materials, as well as with high electric conductivity and corrosion resistance. All developed catalytic inks were benchmarked against the commercial NiFe2O4 catalyst and provided similar or even better performance validating the relevance and competitiveness of the proposed alternatives.

Therefore, although the characterisation was not carried out as expected, using different techniques due to the lack of time for that, the main objective of this project was achieved since several alternative anodes were developed using a simple deposition method through airbrushing technique avoiding harmful solvents and complex procedures. Moreover, the materials used in this project are abundant, corrosion-resistant and highly conductive. This supports the scalability and environmental goals of the project.

6.2 Contribution to the Sustainable Development Goals

Table 5 - Sustainable Development Goals

SDG	Target	Contribution	Performance indicators and metrics
7	7.2	Developing low-cost OER anodes to improve the performance of water and CO_2 electrolysers powered by renewable electricity, contributing to large-scale green hydrogen and eFuel production	Current density achieved ($A \cdot cm^{-2}$), overpotential for OER (V), energy efficiency of electrolyser (%)
13	13.2	Supporting climate change mitigation by developing eFuels from CO_2 and renewable H_2, reducing greenhouse gas emissions in energy and transportation sectors	Development of key enabling technologies (electrodes for CO_2 and water electrolysis) that support carbon-neutral fuel production and CO_2 valorisation

6.3 Final Assessment

The main objective of this project was achieved since alternative anodes for the oxygen evolution reaction were developed and tested in water electrolysis. The procedure proposed (from the ink preparation until the AEM electrolyser tests) in this work was an optimised process of previous works.

Concerning the deposition of the inks, although it is a simple and green method using non-toxic components, it can provide some challenges such as inconsistent deposition of the ink or even if the air pressure is too high it can flood the material not being able to use it for any additional testing. To overcome these issues, an automatic system should be studied and implemented.

Although the batch cell tests are an excellent way to characterise the electrodes, there are some aspects that must be improved, especially during the cell assembling for which the smallest change in the position of the reference and counter electrode can result in different performance making it harder to evaluate.

Regarding the membranes, unfortunately just one kind of membrane was used to test the electrodes. Some future tests would be appreciated by changing the membrane to see if the results maintain or can even be improved.

From my point of view, even with a lot of work to do towards a new sustainable electrolyser system, this project was well carried out. It let me learn more about electrochemistry and work with the latest energy technologies. From creating the ink to testing in the electrolysers, every step provided important information about the problems and possibilities of making OER electrodes that are environmentally friendly. This was an enriching experience that showed me the importance of innovation in creating solutions that are both effective and environmentally friendly for sustainable decarbonisation solutions.

7 References

1. *Record carbon emissions highlight urgency of Global Greenhouse Gas Watch*. Available from: https://wmo.int/media/news/record-carbon-emissions-highlight-urgency-of-global-greenhouse-gas-watch?utm_source=chatgpt.com.
2. *Half of world's CO2 emissions come from 36 fossil fuel firms, study shows*. Available from: www.theguardian.com/environment/2025/mar/05/half-of-worlds-co2-emissions-come-from-36-fossil-fuel-firms-study-shows.
3. Nitopi, S., E. Bertheussen, S.B. Scott, X. Liu, A.K. Engstfeld, S. Horch, B. Seger, I.E.L. Stephens, K. Chan, C. Hahn, J.K. Nørskov, T.F. Jaramillo, and I. Chorkendorff, *Progress and Perspectives of Electrochemical CO2 Reduction on Copper in Aqueous Electrolyte*. Chemical Reviews, 2019. **119**(12): p. 7610-7672.
4. Zhang, J., C. Guo, S. Fang, X. Zhao, L. Li, H. Jiang, Z. Liu, Z. Fan, W. Xu, J. Xiao, and M. Zhong, *Accelerating electrochemical CO2 reduction to multi-carbon products via asymmetric intermediate binding at confined nanointerfaces*. Nature Communications, 2023. **14**(1): p. 1298.
5. *About us*. Available from: https://ceft.fe.up.pt/about/.
6. Leonzio, G., A. Hankin, and N. Shah, *CO2 electrochemical reduction: A state-of-the-art review with economic and environmental analyses*. Chemical Engineering Research and Design, 2024. **208**: p. 934-955.
7. Wiranarongkorn, K., K. Eamsiri, Y.-S. Chen, and A. Arpornwichanop, *A comprehensive review of electrochemical reduction of CO2 to methanol: Technical and design aspects*. Journal of CO2 Utilization, 2023. **71**: p. 102477.
8. Gawel, A., T. Jaster, D. Siegmund, J. Holzmann, H. Lohmann, E. Klemm, and U.-P. Apfel, *Electrochemical CO₂ reduction - The macroscopic world of electrode design, reactor concepts & economic aspects*. iScience, 2022. **25**(4).
9. Chen, Q., P. Tsiakaras, and P. Shen *Electrochemical Reduction of Carbon Dioxide: Recent Advances on Au-Based Nanocatalysts*. Catalysts, 2022. **12**, DOI: 10.3390/catal12111348.
10. Jiang, Y., F. Chen, and C. Xia, *A review on cathode processes and materials for electro-reduction of carbon dioxide in solid oxide electrolysis cells*. Journal of Power Sources, 2021. **493**: p. 229713.
11. An, H., W. Park, H. Shin, and D. Chung, *Recommended practice for measurement and evaluation of oxygen evolution reaction electrocatalysis*. EcoMat, 2024. **6**.
12. Cao, X., Y. Gao, Y. Li, D.M. Weragoda, G. Tian, W. Zhang, Z. Zhang, X. Zhao, and B. Chen, *Research progress on MOFs and their derivatives as promising and efficient electrode materials for electrocatalytic hydrogen production from water*. RSC Advances, 2023. **13**(35): p. 24393-24411.
13. Son, Y.J., K. Kawashima, R.A. Márquez, L.A. Smith, C.E. Chukwuneke, and C.B. Mullins, *Key concepts for understanding alkaline oxygen evolution reaction at the atomic/molecular scale*. Current Opinion in Electrochemistry, 2023. **39**: p. 101298.
14. Görlin, M., P. Chernev, J. Ferreira de Araújo, T. Reier, S. Dresp, B. Paul, R. Krähnert, H. Dau, and P. Strasser, *Oxygen Evolution Reaction Dynamics, Faradaic Charge Efficiency, and the Active Metal Redox States of Ni–Fe Oxide Water Splitting Electrocatalysts*. Journal of the American Chemical Society, 2016. **138**(17): p. 5603-5614.

15. Wu, C., Y. Tang, A. Zou, J. Li, H. Meng, F. Gao, J. Wu, and X. Wang, *Recommended electrochemical measurement protocol for oxygen evolution reaction*. DeCarbon, 2025. **8**: p. 100108.

16. Vass, Á., A. Kormányos, Z. Kószó, B. Endrődi, and C. Janáky, *Anode Catalysts in CO2 Electrolysis: Challenges and Untapped Opportunities*. ACS Catalysis, 2022. **12**(2): p. 1037-1051.

17. Weng, L.-C., A.T. Bell, and A.Z. Weber, *Towards membrane-electrode assembly systems for CO2 reduction: a modeling study*. Energy & Environmental Science, 2019. **12**(6): p. 1950-1968.

18. Habibzadeh, F., P. Mardle, N. Zhao, H.D. Riley, D.A. Salvatore, C.P. Berlinguette, S. Holdcroft, and Z. Shi, *Ion Exchange Membranes in Electrochemical CO2 Reduction Processes*. Electrochemical Energy Reviews, 2023. **6**(1): p. 26.

19. Son, Y.J., G. Mirshekari, S.J. Raaijman, and P.J. Corbett, *Technology Landscape of Anion Exchange Membrane Water Electrolyzers: Where Are We Today?* ACS Energy Letters, 2025: p. 3058-3063.

20. Hagesteijn, K., S. Jiang, and B. Ladewig, *A review of the synthesis and characterization of anion exchange membranes*. Journal of Materials Science, 2018. **53**.

21. Du, N., C. Roy, R. Peach, M. Turnbull, S. Thiele, and C. Bock, *Anion-Exchange Membrane Water Electrolyzers*. Chemical Reviews, 2022. **122**(13): p. 11830-11895.

22. Willdorf-Cohen, S., A. Zhegur-Khais, J. Ponce-González, S. Bsoul-Haj, J.R. Varcoe, C.E. Diesendruck, and D.R. Dekel, *Alkaline Stability of Anion-Exchange Membranes*. ACS Applied Energy Materials, 2023. **6**(2): p. 1085-1092.

23. Bazan-Aguilar, A., G. García, E. Pastor, and A.M. Baena-Moncada, *Highly active NiMo foam-based electrocatalysts for the hydrogen evolution reaction in alkaline media*. Electrochimica Acta, 2024. **479**: p. 143881.

24. Zhu, Q., X. Sun, D. Yang, J. Ma, X. Kang, L. Zheng, J. Zhang, Z. Wu, and B. Han, *Carbon dioxide electroreduction to C2 products over copper-cuprous oxide derived from electrosynthesized copper complex*. Nature Communications, 2019. **10**(1): p. 3851.

25. Daly, K.M., S. Jimenez-Villegas, B. Godwin, M.A.W. Schoen, O. Calderon, N. Chen, and S. Trudel, *A Comparison of Photodeposited RuOx for Alkaline Water Electrolysis*. ACS Applied Energy Materials, 2023. **6**(3): p. 1449-1458.

26. Liu, W., Z. Hu, T. Ren, Z. Xiang, J. Piao, K. Wan, Z. Fu, and Z. Liang, *Efficient and robust single-layer IrOx cluster electrocatalyst for oxygen evolution reaction*. Chemical Engineering Science, 2024. **299**: p. 120508.

27. McCrory, C.C.L., S. Jung, J.C. Peters, and T.F. Jaramillo, *Benchmarking Heterogeneous Electrocatalysts for the Oxygen Evolution Reaction*. Journal of the American Chemical Society, 2013. **135**(45): p. 16977-16987.

28. Morais, D.F.S., J.C.B. Lopes, M.M. Dias, V.J.P. Vilar, and F.C. Moreira, *e-NETmix: A pioneering electrochemical flow reactor with enhanced mass transfer*. Chemical Engineering Journal, 2024. **481**: p. 148244.

29. Atobe, M., H. Tateno, and Y. Matsumura, *Applications of Flow Microreactors in Electrosynthetic Processes*. Chemical Reviews, 2018. **118**(9): p. 4541-4572.

30. Wang, W., Z. Wu, D. Peters, B. Citmaci, C.G. Morales-Guio, and P.D. Christofides, *Machine learning in modeling, analysis and control of electrochemical reactors: A tutorial review*. Digital Chemical Engineering, 2025. **15**: p. 100237.

31. Dafeng, Y., C. Asmelash, S. Wang, and R. Palkovits, *Innovative Electrochemical Strategies for Hydrogen Production: From Electricity Input to Electricity Output*. Angewandte Chemie, 2022. **135**.

32. Angulo, A., P. van der Linde, H. Gardeniers, M. Modestino, and D. Fernández Rivas, *Influence of Bubbles on the Energy Conversion Efficiency of Electrochemical Reactors.* Joule, 2020. **4**(3): p. 555-579.

33. Noël, T., Y. Cao, and G. Laudadio, *The Fundamentals Behind the Use of Flow Reactors in Electrochemistry.* Accounts of Chemical Research, 2019. **52**(10): p. 2858-2869.

34. Ince, M.C., B. Benyahia, and G. Vilé, *Sustainability and Techno-Economic Assessment of Batch and Flow Chemistry in Seven Industrial Pharmaceutical Processes.* ACS Sustainable Chemistry & Engineering, 2025. **13**(7): p. 2864-2874.

35. Wu, T., B. Liu, H. Hao, F. Yuan, Y. Zhang, H. Tan, and Q. Yang, *Coalescence-induced late departure of bubbles improves water electrolysis efficiency*. 2024.

36. Ralph, T.R., M.L. Hitchman, J.P. Millington, and F.C. Walsh, *The electrochemistry of l-cystine and l-cysteine part 2 : Electrosynthesis of l-cysteine at solid electrodes.* Journal of Electroanalytical Chemistry, 1994. **375**(1): p. 17-27.

37. Jung, S., C.C.L. McCrory, I.M. Ferrer, J.C. Peters, and T.F. Jaramillo, *Benchmarking nanoparticulate metal oxide electrocatalysts for the alkaline water oxidation reaction.* Journal of Materials Chemistry A, 2016. **4**(8): p. 3068-3076.

38. Chen, F.-Y., Z.-Y. Wu, Z. Adler, and H. Wang, *Stability challenges of electrocatalytic oxygen evolution reaction: From mechanistic understanding to reactor design.* Joule, 2021. **5**(7): p. 1704-1731.

39. Zeradjanin, A.R., J. Masa, I. Spanos, and R. Schlögl, *Activity and Stability of Oxides During Oxygen Evolution Reaction---From Mechanistic Controversies Toward Relevant Electrocatalytic Descriptors.* Frontiers in Energy Research, 2021. **Volume 8 - 2020**.

40. Yamada, H., K. Yoshii, M. Asahi, M. Chiku, and Y. Kitazumi, *Cyclic Voltammetry Part 2: Surface Adsorption, Electric Double Layer, and Diffusion Layer.* Electrochemistry, 2022. **90**(10): p. 102006-102006.

41. Yamada, H., K. Yoshii, M. Asahi, M. Chiku, and Y. Kitazumi, *Cyclic Voltammetry Part 1: Fundamentals.* Electrochemistry, 2022. **90**(10): p. 102005-102005.

42. Marquez, R.A.a.M., C. Buddie. *Using Cyclic Voltammetry to Detect Iron Impurities During Water Oxidation Measurements*. 2025.

43. Elgrishi, N., K.J. Rountree, B.D. McCarthy, E.S. Rountree, T.T. Eisenhart, and J.L. Dempsey, *A Practical Beginner's Guide to Cyclic Voltammetry.* Journal of Chemical Education, 2018. **95**(2): p. 197-206.

44. Kubo, N., F. Ketter, S. Palkovits, and R. Palkovits, *Nickel and Commercially Available Nickel-Containing Alloys as Electrodes for the Electrochemical Oxygen Evolution.* ChemElectroChem, 2024. **11**.

45. Jović, V., *Calculation of a pure double-layer capacitance from a constant phase element in the impedance measurements.* Zastita materijala, 2022. **63**: p. 50-57.

46. Sun, Z., T. Du, Y. Li, H. Jia, Q. Yue, H. Wang, and Y. Wang, *Cu-Dopant in nickel-based hydrotalcite-derived catalysts for low temperature CO2 methanation.* Materials Today Energy, 2025. **52**: p. 101941.

47. Hall, D., D. Lockwood, C. Bock, and B. MacDougall, *Nickel hydroxides and related materials: A review of their structures, synthesis and properties.* Proceedings of The Royal Society A Mathematical Physical and Engineering Sciences, 2015. **471**: p. 1-65.

Annex A - Supplementary information for the analysis of the electrochemical results

In this section, the complementary information and results are presented.

A.1 Characterisation Results

Dynamic Light Scattering

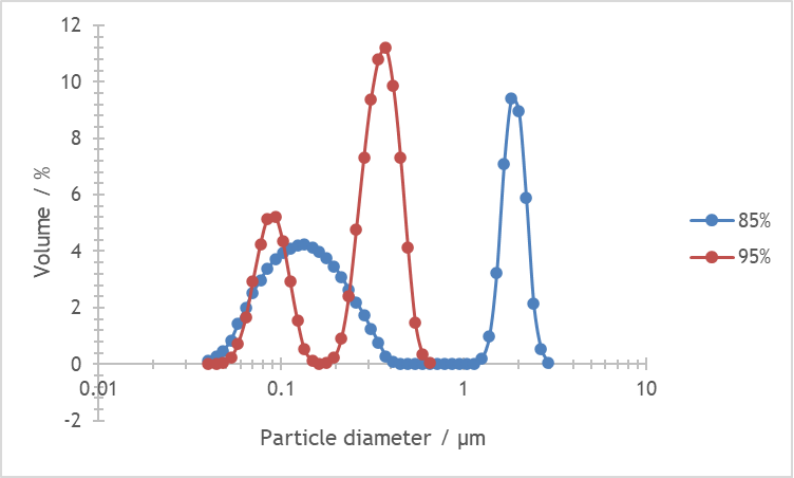

Figure A.1 - Characterisation results for the 95 % and 85 % nickel-based inks in DLS

The particle size distribution analysis reveals that sample 85 Ni exhibits a bimodal profile with a dominant peak around 2 µm, while 95 Ni shows a narrower distribution centered near 0.5 µm, indicating significantly smaller and more uniform particles.

X-Ray diffraction

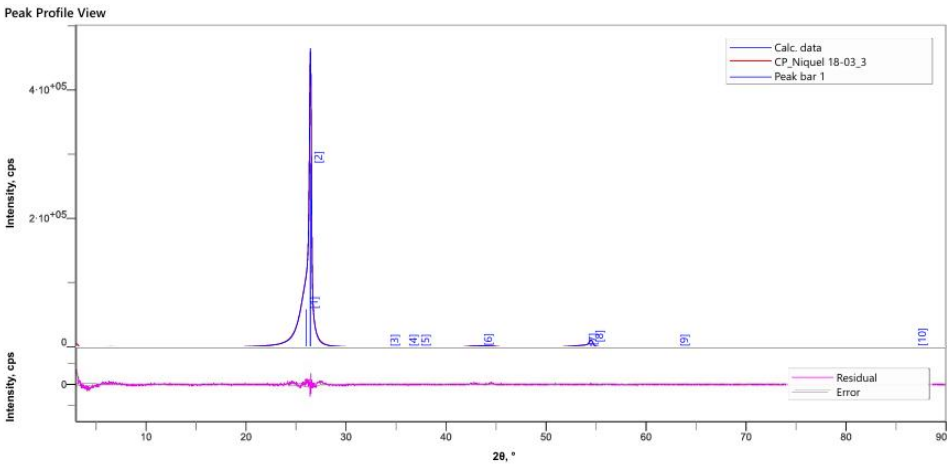

Figure A.2 - XRD results for nickel supported on silica/alumina

Due to the strong diffraction signal from the carbon paper substrate, which dominated the initial scan (0–90°), a second scan was conducted over a narrower range (30–90°) to improve the visibility of weaker peaks associated with the deposited materials.

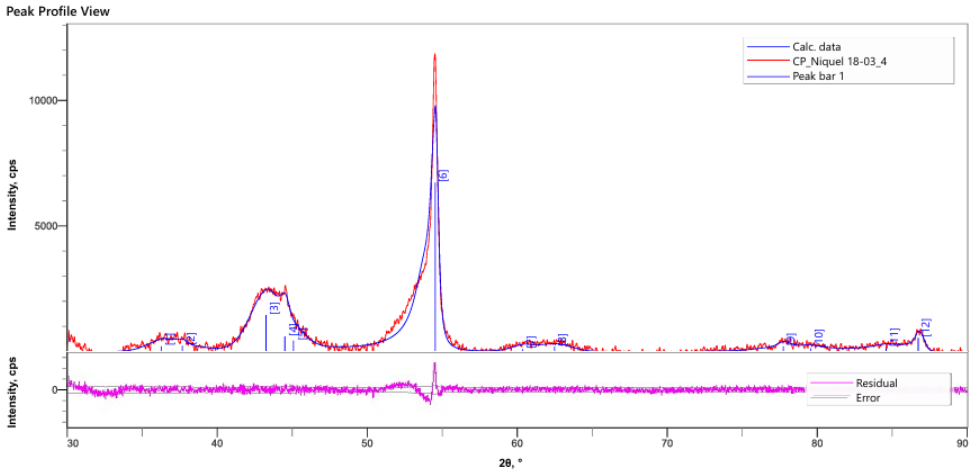

Figure A.3 - Repetition of the XRD tests for nickel supported on silica/alumina

Despite the overall low peak intensities, several characteristic reflections were identified at positions consistent with those of nickel (Ni) and nickel oxide (NiO), based on standard JCPDS reference values. Specifically, peaks corresponding to the (111) and (200) planes of both Ni and NiO were detected at approximately 37.2°, 43.2°, 44.6°, and 51.7°, confirming the presence of both metallic and oxidized nickel species in the sample. Given that all inks were deposited using the same methodology, and that the XRD data confirms the presence of the intended crystalline phases in the representative Ni/SiO_2–Al_2O_3 ink, the deposition process can be considered validated across all formulations.

A.2 Voltammograms and respective scan rate tests for each formulation

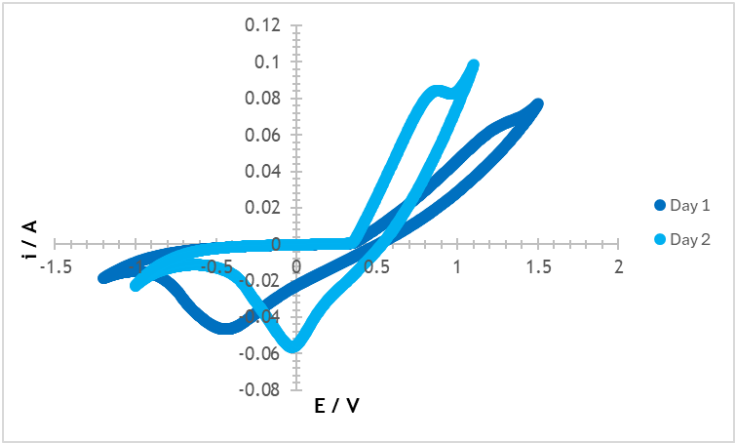

Figure A.4 - Voltammograms obtained for the electrodes loaded with 95 % Nickel(II) nitrate hexahydrate and 5 % Copper (I) oxide deposited

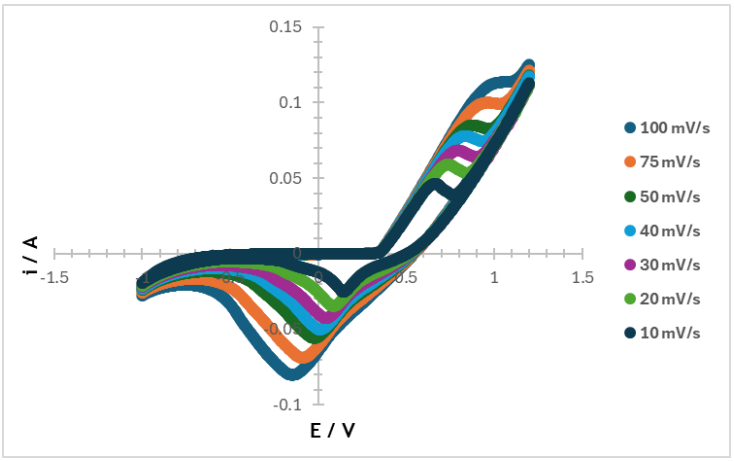

Figure A.5 - Scan rate results at the Faradaic zone of the voltammogram

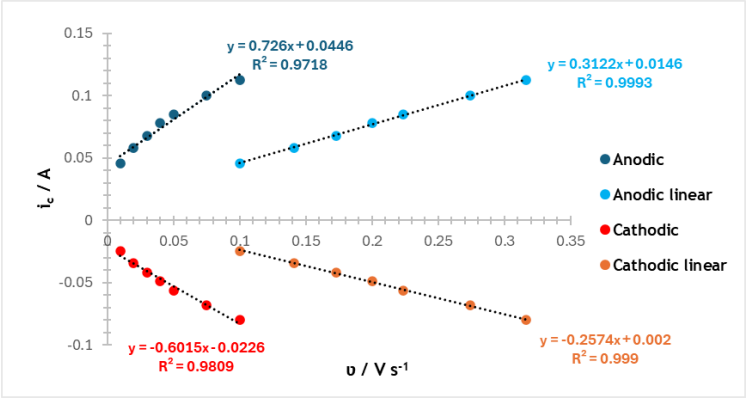

Figure A.6 - Linearization of the i vs υ plots

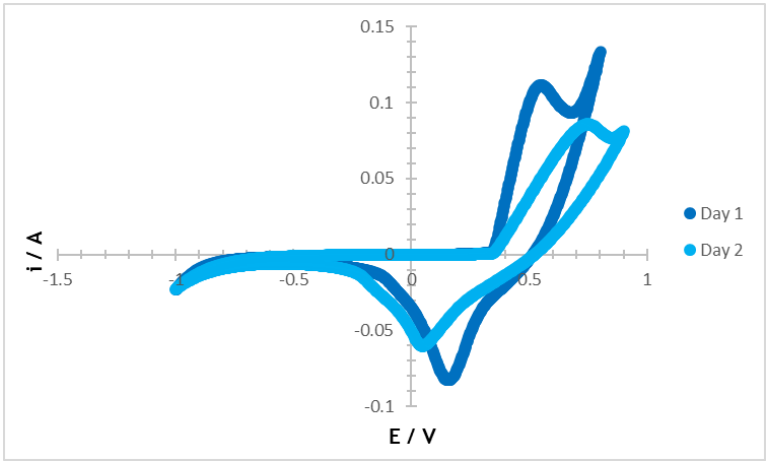

Figure A.7 - Voltammograms obtained for the electrodes loaded with 90 % Nickel(II) nitrate hexahydrate and 10 % Copper (I) oxide deposited

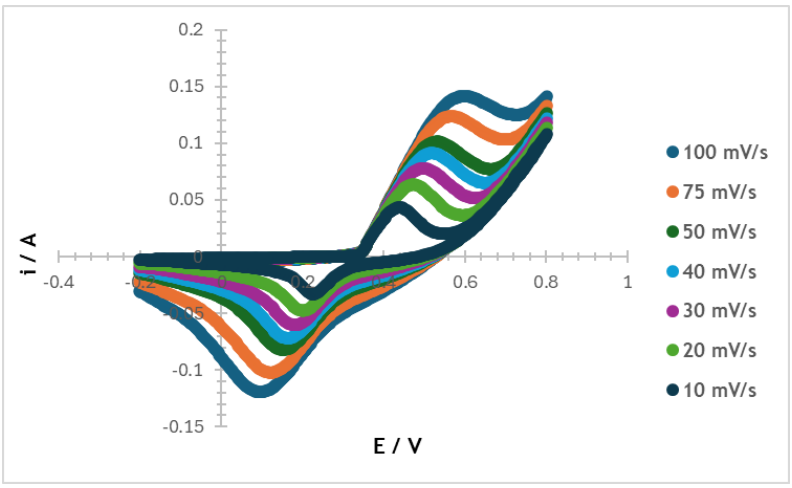

Figure A.8 - Scan rate results at the Faradaic zone of the voltammogram

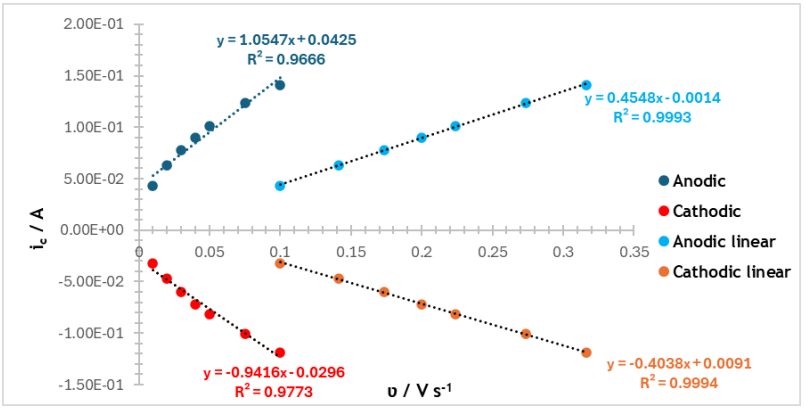

Figure A.9 - Linearization of the i vs υ plots

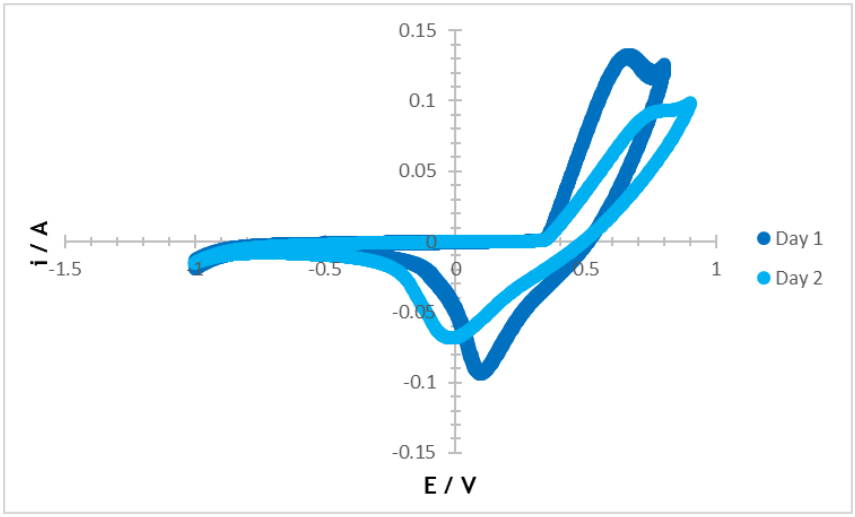

Figure A.10 - Voltammograms obtained for the electrodes loaded with 85 % Nickel(II) nitrate hexahydrate and 15 % Copper (I) oxide deposited

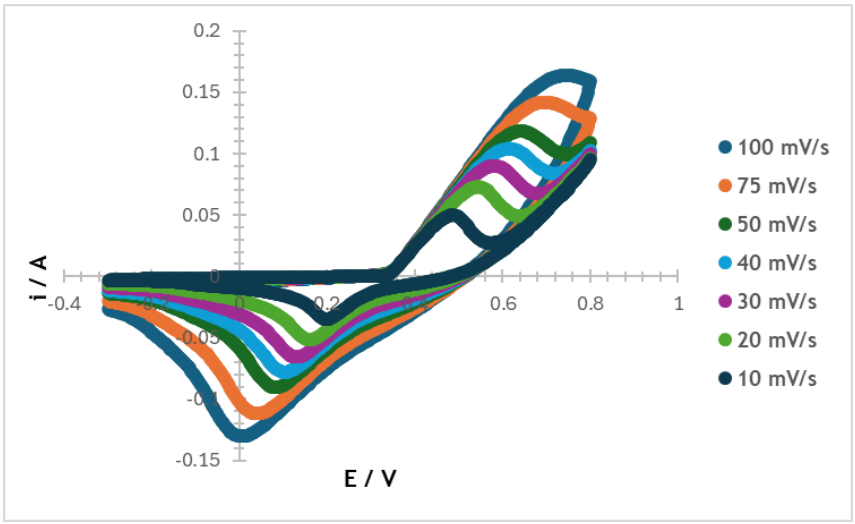

Figure A.11 - Scan rate results at the Faradaic zone of the voltammogram

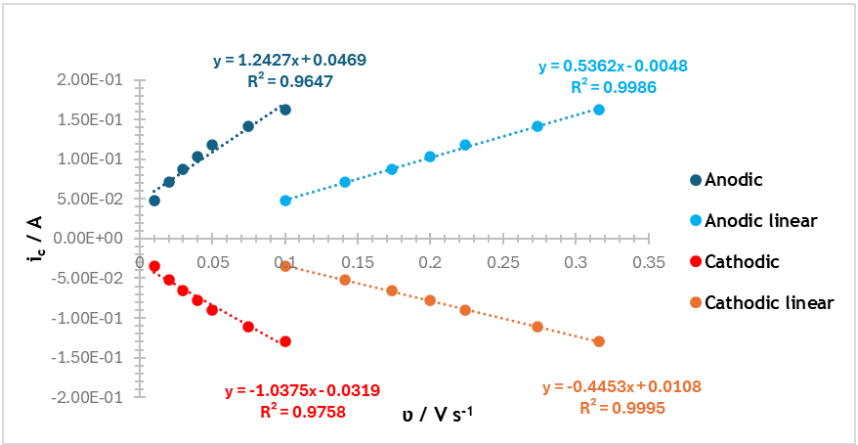

Figure A.12 - Linearization of the i vs υ plots

A.3 Baseline validation

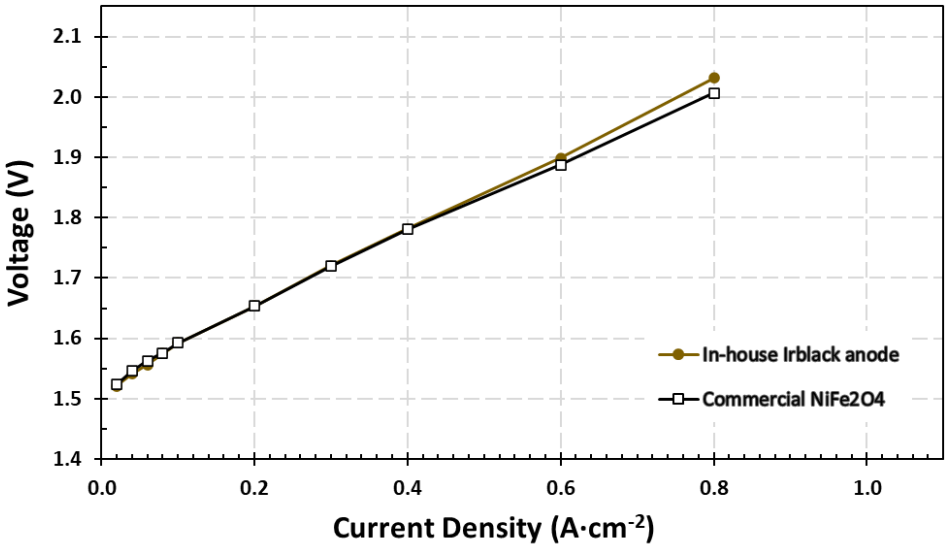

Figure A.13 - Comparison of the commercial's polarisation curves

A.4 Electrolyser assembly

To assemble and prepare the electrolyser for testing, following these steps were essential:

1. Always wear protective gloves during handling.
2. Use a template to cut the membrane and submerge it in a 1 M KOH bath for 24 hours.
3. Disconnect and disassemble the electrolyser. Clean all components thoroughly with distilled water, using a brush if needed.
4. Remove the membrane, peel off any protective layers, dry it using paper towels, and let it sit for 10 minutes.
5. Cut the electrodes to 2.2 cm × 2.2 cm to match the membrane's active area and punch two alignment holes.
6. Assemble the stack in this sequence: anode end plate → external gasket → anode bipolar plate → anode-side gasket → anode electrode → membrane → cathode-side gasket → cathode electrode → cathode bipolar plate → external gasket → cathode end plate.
7. Insert and lightly hand-tighten all bolts, then torque them sequentially in a crisscross pattern using four steps: 0.5, 1.0, 2.0, and 3.0 Nm.
8. Perform an electrical continuity test and both external (1 bar N_2, pressure drop < 0.05 bar in 10 min) and internal leak tests (0.3 bar N_2 on the anode side, check for bubbles on cathode submerged in water).

9. Reconnect the electrolyser to the system.

A.5 Electrolyser operation procedure

Startup and execution:

1. Ensure all equipment is off and launch the LabVIEW control software.
2. Check tubing, electrode alignment, thermocouple placement, and fill the storage tank with sufficient electrolyte. Turn on the stirrer and heater.
3. Start the peristaltic pump in forward flow mode. Adjust the temperature carefully, allowing time between increases.
4. Once stable, power on the DC supply and conduct a stress test: increase current until 2.435 V, then hold at 2.0 V for 2 hours to activate the membrane.
5. Launch the I-V acquisition program. It applies current in steps (0.02 $A \cdot cm^{-2}$ increments up to 0.1 $A \cdot cm^{-2}$, then 0.1 $A \cdot cm^{-2}$ steps), stopping at 2.0 V. Repeat until reproducible results are obtained.

Shutdown Procedure:

6. Save the data, set temperature to zero, stop the programs, and turn off the DC power and pump.
7. Power down the entire setup and ensure all systems are off.